

Odour-evoked $[Ca^{2+}]$ transients in mitral cell dendrites of frog olfactory glomeruli

Kerry Delaney,¹ Ian Davison¹ and Winfried Denk²

¹Department of Biological Sciences, Simon Fraser University, 8888 University Drive, Burnaby, B.C. V5A 1S6, Canada

²Biological Computation Research Department, Bell Laboratories, Lucent Technologies, Murray Hill, NJ, 07974, USA

Keywords: calcium imaging, frog, NMDA receptors, olfactory bulb, *Rana pipiens*, two-photon scanning laser microscopy

Abstract

We measured Ca^{2+} concentration, $[Ca^{2+}]$, transients in mitral cell distal apical dendritic tufts produced by physiological odour stimulation of the olfactory epithelium and electrical stimulation of the olfactory nerve (ON) using two-photon scanning and conventional wide-field microscopy of Ca^{2+} -Green-1 dextran in an *in vitro* frog nose–brain preparation. Weak or strong ON shock-evoked fluorescence transients always had short latency with an onset 0–10 ms after the onset of the bulb local field potential, rapidly increasing to a peak of up to 25% fractional fluorescence change ($\Delta F/F$) in 10–30 ms, were blocked by 10 μM CNQX, decaying with a time constant of about 1 s. With stronger ON shocks that activated many receptor axons, an additional, delayed, sustained AP5-sensitive component (peak at ≈ 0.5 s, up to 40% $\Delta F/F$ maximum) could usually be produced. Odour-evoked $[Ca^{2+}]$ transients sometimes displayed a rapid onset phase that peaked within 50 ms but always had a sustained phase that peaked 0.5–1.5 s after onset, regardless of the strength of the odour or the amplitude of the response. These were considerably larger (up to 150% $\Delta F/F$) than those evoked by ON shock. Odour-evoked $[Ca^{2+}]$ transients were also distinguished from ON shock-evoked transients by tufts in different glomeruli responding with different delays (time to onset differed by up to 1.5 s between different tufts for the same odour). Odour-evoked $[Ca^{2+}]$ transients were increased by AMPA-kainate receptor blockade, but substantially blocked by AP5. Electrical stimulation of the lateral olfactory tract (5–6 stimuli at 10 Hz) that evoked granule cell feedback inhibition, blocked 60–100% of the odour-evoked $[Ca^{2+}]$ transient in tufts when delivered within about 0.5 s of the odour. LOT-mediated inhibition was blocked by 10 μM bicuculline.

Introduction

This paper presents experiments using an *in vitro* preparation of frog nose and forebrain (Delaney & Hall, 1996) in which we have studied Ca^{2+} concentration, $[Ca^{2+}]$, dynamics in mitral cell (MC) distal apical tufts and apical dendritic shafts to probe the function of this dendritic compartment in the olfactory glomerulus. We used fluorescence imaging to observe $[Ca^{2+}]$ transients produced by natural physiological stimulation of the sensory epithelium with odours, and compared this with artificial electrical stimulation of the olfactory nerve (ON) and lateral olfactory tract (LOT).

Much of our knowledge of olfactory bulb (OB) physiology, including the pharmacology of the sensory afferent input (Berkowicz *et al.*, 1994; Ennis *et al.*, 1996) and the theoretical framework for network-level activities such as odour-evoked oscillations (Rall & Shepherd, 1968), is derived from study of orthodromic electrical stimulation of the ON or nasal epithelium and antidromic stimulation of the MC axons in the LOT. We know, however, that stimulation of the olfactory bulb circuitry with odours elicits neural activity that is qualitatively different from ON stimulation. Odour characteristically induces bouts of oscillatory activity in the intact olfactory bulb (Adrian, 1942; Hobson, 1967; Tank *et al.*, 1994; Delaney & Hall, 1996; Lam *et al.*, 2000) whereas orthodromic stimulation of the ON produces synchronized excitation of many MCs, followed by strong

feedback inhibition that suppresses evoked and spontaneous activity for several seconds (Jahr & Nicoll, 1982). Differences between odour- and nerve shock-evoked activity of the OB presumably arise from the differences in the spatiotemporal pattern of olfactory inputs that each activates. Therefore, further studies in which odours are used to activate OB networks are needed to complement a recent resurgence in electrophysiological analysis using OB brain slices (Aroniadou-anderjaska *et al.*, 1997, 1999; Bischofberger & Jonas, 1997; Chen *et al.*, 1997; Isaacson & Strowbridge, 1998; Kirillova & Lin, 1998; Puopolo & Belluzzi, 1998; Schoppa *et al.*, 1998; Isaacson, 1999). We developed the *in vitro* nose–brain preparation of frog in order to bridge the gap between brain slice and *in vivo* experiments.

Central to the difference between ON shock and odour stimulation is the functional convergence of olfactory receptor neurons. Peripheral olfactory receptor neurons (ORNs) project to anatomically distinct glomerular structures in the OB. Molecular studies indicate that, at least in mammals, ORNs expressing RNA for the same putative receptor protein converge onto one or at most a few glomeruli in the main olfactory bulb (Ressler *et al.*, 1994; Vassar *et al.*, 1994). This implies that afferents with similar odour sensitivity converge onto specific glomeruli. Physiological demonstration of this anatomically identified convergence is supported by 2-deoxyglucose, voltage-sensitive dye, fluorescent Ca^{2+} imaging and reflectance studies (Cinelli *et al.*, 1995; Friedrich & Korsching, 1997; Bozza & Kauer, 1998; Rubin & Katz, 1999) in several species. ORNs respond to application of odourants with repetitive firing over the course of a second or more, and the time of onset and rate of firing of action

Correspondence: Dr Kerry Delaney, as above.
E-mail: kdelaney@sfu.ca

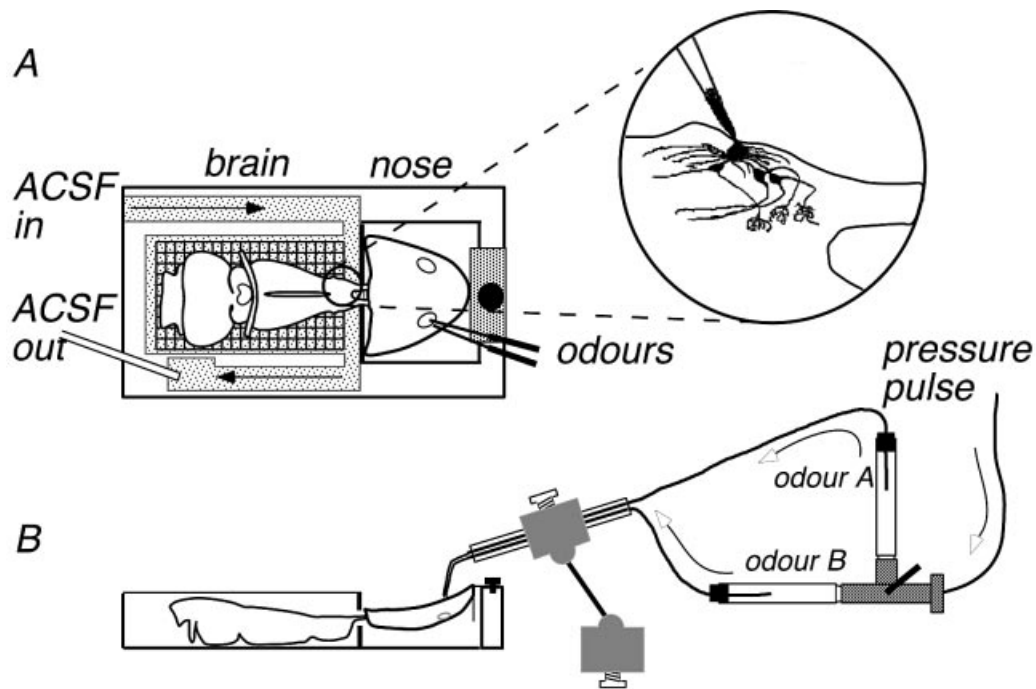


FIG. 1. (A and B) Top and side views of the nose–brain preparation. The nose is maintained in air separated from the brain by a grease-filled gap in the wall through which the olfactory nerve pass. The inset in A illustrates the point of application of Ca^{2+} -Green-1 dextran conjugate coated to the outside of a glass micropipette and how tufts were filled via the secondary dendrites of the mitral cells.

potentials in an ORN reflects odour species and concentration (Getchell, 1986). On the other hand, a single electrical stimulation of the ON evokes a single simultaneous action potential in many ORN axons projecting to glomeruli in all regions of the bulb. Thus, the spatial and temporal patterns of excitation (and subsequent feedback inhibition of MCs) produced by an odour stimulation differ substantially from those produced by ON or epithelium.

Besides the ORN terminals, olfactory glomeruli also contain distal apical dendritic tufts of mitral and tufted cells, and dendrites of several types of short axon periglomerular cells (PG) surrounded by encapsulating glial cells (Shepherd & Greer (1990). Physiological study of these distinct structures, including the role of MC dendritic tufts and PG–MC reciprocal dendrodendritic synapses for inter- and intraglomerular processing (Freeman, 1974; Getchell & Shepherd, 1975; Schild & Riedel, 1992), has been limited by the small size of the PG neurons and the thin branches of the MC apical tufts. To complement electrophysiological analysis, we have turned to fluorescence imaging of Ca^{2+} indicators in MC dendritic tufts during odour stimulation.

The study of Ca^{2+} influx and removal, and the modulation of these processes in MC dendritic tufts, is particularly germane to understanding the role of this neuronal compartment in local circuit function because the MC tuft releases neurotransmitter onto PG neurons. Furthermore, the ON-evoked synaptic potential has contributions from both α -amino-3-hydroxy-5-methyl-4-isoxazolepropionic acid (AMPA) -kainate and N-methyl-D-aspartate (NMDA) -type glutamate receptors (Berkowicz *et al.*, 1994). Thus, there is potential for Ca^{2+} influx through ligand-gated and voltage-gated channels so that Ca^{2+} imaging can provide information about synaptic and electrical processes in these dendrites. We demonstrate that the odour-evoked $[\text{Ca}^{2+}]$ transient in the distal apical dendrite is mostly dependent on activation of NMDA-type receptors (NMDA-R), and

not dependent on AMPA-kainate-R whereas the ON shock-evoked response is dominated by AMPA-kainate-R. Evidence that inhibitory synaptic inputs can significantly downregulate the odour-evoked Ca^{2+} influx into the distal dendrite is presented and the possibility that this is related directly to the differences between odour and ON shock-evoked activity in the bulb is explored. Some of these results have been presented in abstract form (Davison & Delaney, 1997, 1998, 2000; Delaney & Denk, 1996).

Methods

Dissection and electrophysiology

The preparation and physiological characterization of the *in vitro* nose–brain of *Rana pipiens* is described in detail in Delaney & Hall (1996). Frogs were cryoanaesthetized to a state of torpor and, following rapid decapitation, the brain anterior to the tectum was removed from the cranium retaining the ON connected to the olfactory epithelium that is enclosed within the nasal cavity. The brain was submerged in frog Ringer equilibrated with 95%/5% O_2/CO_2 while the nose was placed in a separate chamber to permit application of air-borne odourants (Fig. 1). Frogs were housed at room temperature while the *in vitro* brain was maintained at around 19 °C using a stage-mounted peltier device. Odourants were delivered to the nose using brief (5–300 ms) air pressure pulses (0.7–13.8 kPa, i.e. 0.1–2 p.s.i.), monitored with a digital pressure meter (Sensym, SCX-LCD, Sunnyvale, CA, USA) applied to the odour reservoirs. The reservoirs were made from 1-mL syringes containing filter paper soaked in odourants (*n*-butanol, methyl salicylate or isoamyl acetate), prepared by dilution (1 : 100–1 : 10 000 v/v) of pure stocks in water followed by 5 min of sonication. To direct the odour puffs over the epithelia, the tips of

syringe needles (25 gauge, 1.5 cm long) attached to the reservoirs for the two odours to be used in the experiment were placed at the internal opening of the nares (Fig. 1). The puffer delivered small volumes, 0.1 mL or less, of odourant into the nasal cavity. The openings of the external nares were enlarged slightly to facilitate air exchange through the nose, but a continuous stream of air was not applied before or after an odour puff. Thus, although the puffs of air were brief compared with the duration of the local field potential (LFP), odourants were resident in the nasal chamber after the puff offset. The interval between sequential odour applications was always at least 1 min to allow effects of prior odour applications to disappear, as judged by the repeatability of evoked bulb LFP and dendritic $[Ca^{2+}]$ transient.

The odour stimulation ranged from short pulses that elicited a barely detectable LFP to long pulses to which a full bout of odour-evoked oscillations were seen (see also Delaney & Hall, 1996). Increasing the pressure of the air pulse over the range 0.7–13.5 kPa had effects similar to changing the duration, but it was more difficult to achieve repeatable fine adjustment of the pressure of the air pulse, so for all the data presented here puff duration was varied while holding pressure constant, usually at around 10.5 kPa. Quantitative estimates of the concentration of odour inside the nasal cavity were not possible with our apparatus, but they were not necessary for the purposes of this study. Instead the effective strength of the odour stimuli used in an experiment was defined in terms of the LFP they elicited with respect to the maximal odour-evoked LFP. For example, once a tuft was found that responded to an odour stimulus strong enough to evoke a near maximal LFP response, the puff duration was reduced until a small LFP response was produced, to define the range of odour stimuli corresponding with 'weak' to 'strong' odour stimulation. 'Weak' to 'strong' ON shock stimuli were similarly defined based on the amplitude of the LFP they evoked.

LFP responses were recorded from the bulb using Ringer-filled glass micropipettes ($R \approx 5 \text{ M}\Omega$). The electrode tip was positioned approximately 200–300 μm below the bulb surface, i.e. within the region where MC somata and apical dendrites predominate, usually within the anterior half of the bulb so the afferent volley was a small component of the response. The LFP was used as a temporal marker when comparing the time to onset of $[Ca^{2+}]$ transients for different stimulation intensities and between tufts. Since the MCs in frogs are not arranged in a narrow layer as they are in mammals, the LFP waveform does not show a sharp reversal or dramatic change in form with depth in the OB once the electrode is positioned $>100 \mu\text{m}$ below the glomerular layer. However, because of potential variation in LFP location between preparations, we limited quantitative comparison of $[Ca^{2+}]$ transient onset between tufts to measurements made within the same preparation with the LFP electrode located at one position.

For two-photon laser scanning microscopy (TPLSM) experiments, the output of the LFP amplifier was low-pass filtered at 100 Hz and recorded simultaneously with the fluorescence by encoding the voltage onto the first few pixels of each scan line to ensure precise temporal synchronization of electrophysiological and optical signals. Consequently, sampling frequency for the LFP was typically 500 Hz (the line scan rate). For the studies using aperture-limited spot illumination rather than TPLSM, the LFP and optical signals were low-pass filtered at 1 kHz prior to digitization. Electrical stimulation of the ON or lateral olfactory tract was achieved using pairs of TeflonTM-insulated silver or tungsten wires. An intracellular solution comprised of (in mM) 110 K-gluconate, 8 NaCl, 2 MgCl₂, 0.2 CaCl₂, 1 EGTA, 10 Glucose, 5 HEPES and 0.1 ATP was used for whole-cell recordings of MCs.

Filling mitral cell tufts with Ca^{2+} indicator

Ca^{2+} -Green-1 10 000-MW dextran conjugate (Molecular Probes, Eugene, OR, USA) was applied locally to the lateral surface of the bulb *in vitro* in order to fill MCs (Gelperin & Flores, 1997). A small crystal of dye, 1 mg or less, was dissolved in 1–2 μL of 1.5% bovine serum albumin or 30% sucrose in a well slide and then air dried. A droplet of distilled water, about 0.5 μL , was placed on the dried dye. Fine glass micropipettes were coated with a film of dye by passing them through the edge of the droplet where the dye was highly concentrated and viscous, and then allowing the dye to dry on the pipette. The level of the saline covering the brain was lowered briefly so the dye could be applied to a small portion of the bulb by insertion of 2–4 dye-coated pipettes to a depth of 100–200 μm below the lateral surface of the bulb in an area within 200 μm of the rostral edge of the accessory olfactory bulb (Fig. 1). The tip of each pipette was held in place for about 5 s to allow the dye to dissolve. The region where the dye was applied has no overlying glomeruli, is composed almost exclusively of dendrites of mitral and granule cells and has been termed the 'superficial plexiform layer' (Scalia *et al.*, 1991). The dye was allowed to diffuse for about 2 h before imaging. With this loading method it is not possible to strictly control the concentration of dye in the neurons, but for our measurements we used tufts of similar absolute intensity suggesting fairly comparable dye loading. While a high Ca^{2+} buffer capacity can slow the rate of rise, prolong the recovery and reduce the $\Delta[Ca^{2+}]$ resulting from a brief influx of Ca^{2+} , the onset time of transients evoked by different stimuli would not be affected. It would also not substantially change interpretation of the main differences in $[Ca^{2+}]$ dynamics that we observed with different stimuli. For example, slow-rising, slow-decaying, large-amplitude $[Ca^{2+}]$ transients observed in response to an odour stimulation cannot be due to an artefact of excessive dye loading if in the same cell an electrical ON shock produces a rapidly rising, rapidly decaying response (Tank *et al.*, 1995).

Two-photon-excitation fluorescence imaging

Two-photon fluorescence excitation was achieved using a custom-built laser scanning microscope employing a femtosecond Titanium-Sapphire laser (Tsunami; Spectra Physics, or NJA-2, Clark Instrumentation) to excite Ca^{2+} -Green-1 fluorescence via two-photon excitation (Denk *et al.*, 1990, 1995; Denk & Svoboda, 1997). The excitation wavelength was 830 nm and the average power at the objective lens was up to 200 mW for the deepest dendrites imaged. Whole-field detection (Denk *et al.*, 1995) was used throughout to make efficient use of scattered fluorescent light (Denk, 1996). Fluorescence changes reported here were obtained from square measurement boxes encompassing about 75% of the filled area of the tuft(s) in a glomerulus (e.g. Fig. 4). Fluorescence changes were calculated by subtracting the average intensity of pixels within an area or along a line segment covering the dendrites measured during the 1 s prior to the onset of odour or electrical stimulation (F_{pre}), from the fluorescence in each image or line (F). These changes were then normalised by dividing by F_{pre} after subtracting a background fluorescence (F_{bgnd}), that was estimated from an area or line segment lacking dye-filled structures. Values were expressed as fractional percentage changes, that is, $\% \Delta F/F = (F - F_{\text{pre}})/(F_{\text{pre}} - F_{\text{bgnd}}) \times 100$. By maintaining low excitation light intensity it was possible to obtain fluorescence measurements in response to several odour or shock stimuli without bleaching the dye by more than a few percent. Consequently it was not necessary to correct the TPLSM data for bleaching during a trial. Measurements of dye fluorescence from artificial ringer solutions containing 0 Ca^{2+} and saturated Ca^{2+}

indicated a $\Delta F/F$ of about 400%. The dissociation constant (k_d) for the dye was 250 nM in 100 mM KCl according to the manufacturer. Assuming similar characteristics for the dye in the dendrite and a resting $[\text{Ca}^{2+}]$ of 50 nM, the change in $[\text{Ca}^{2+}]$ can be estimated theoretically from $\Delta F/F$ measurements using the relationship $[\text{Ca}^{2+}] = K_d \times (F - F_0)/(F_{\text{sat}} - F)$ where F_{sat} is the fluorescence at saturating $[\text{Ca}^{2+}]$ and F_0 is the fluorescence at zero $[\text{Ca}^{2+}]$. However, because both the peak fluorescence changes in response to odour were large enough to suggest significant saturation of the indicator and because we had no independent means of assessing resting $[\text{Ca}^{2+}]$ or the *in vivo* Ca^{2+} affinity of the dye, we did not attempt to calibrate our signals beyond commenting on the possible range of $\Delta[\text{Ca}^{2+}]$ and report all optical data as simply $\% \Delta F/F$.

Glutamate pharmacology of $[\text{Ca}^{2+}]$ transients

To investigate the pharmacology of the $[\text{Ca}^{2+}]$ transients, we used conventional wide-field fluorescence microscopy. A stabilized Xe arc lamp (Optiquip Corp., Highland Mills, NY, USA) was used to excite Ca^{2+} -Green-1 dextran (filter set number 41001, Chroma Corp., Brattleboro, VT, USA), and emitted fluorescence detected using a photomultiplier tube (model H5783-03, Hamamatsu, Bridgewater, NJ, USA). To restrict fluorescence measurements to dendrites in a single glomerulus, we used a 60 \times , 0.8 NA, water immersion objective (Olympus Optical), and closed the field aperture to illuminate a small region in the centre of the field of view containing one filled glomerulus. We selected tufts that were separated from other filled structures, towards the edge or caudal portion of the bulb to further reduce out-of-focus fluorescence from other filled dendrites. Non-NMDA receptors were blocked with 10 μM 6-cyano-7-nitroquinoxaline-2,3-dione (CNQX), NMDA receptors were blocked with 50–100 μM AP5 (2-amino-5-phosphonopentanoic acid) (Precision Biochemical, North Vancouver, Canada) and GABA_A receptors were blocked with 10 μM bicuculline methiodide (Sigma, St Louis, MO, USA).

Results

Morphology

In frogs the glomeruli are mainly distributed around the circumference of the anterior part of the bulb where they form a 'cap'. There are glomeruli in the rostral and caudal parts of the bulb on the ventral surface, but only in the rostral portions of the dorsal surface and none on the lateral surface (Scalia *et al.*, 1991). Localized application of dye to the lateral surface of the main olfactory bulb, at a point near the anterior edge of the accessory olfactory bulb, resulted in dye-filled tufts that were distributed across most of the ventral surface of the ipsilateral hemibulb, as well as in the dorsal and ventral parts of the rostral cap (Fig. 2). The orientation of the nose–brain preparation in the recording chamber prevented imaging tufts on the dorsal and ventral surfaces of the most rostral parts of the bulb during odour stimulation. Most of our measurements were made from tufts located 50–150 μm below the ventral surface, 400–700 μm anterior to the dye application site. Before entering a glomerulus, the majority of apical dendrites projected at a shallow angle or perpendicular to the surface within the glomerular layer for at least 50–100 μm , running along the rostrocaudal axis. $[\text{Ca}^{2+}]$ dynamics were examined in tufts in 110 glomeruli in 25 nose–brain preparations using TPLSM and for this study.

Dye-filled tufts appeared as either rather tight dendritic clusters with numerous varicosities or, more commonly, sparsely branched, extended, varicose structures between 10 and 50 μm across (Fig. 2).

Based on differences in dendritic morphology that were correlated with the depth of the somata below the glomerular layer, Jiang and Holley (1992a) proposed that there are two classes of mitral cells in frog that are analogous to the mitral and the tufted mitral classes of mammalian OB. We could not follow dendrites from the tufts from which we had gathered data on $[\text{Ca}^{2+}]$ dynamics back to their corresponding somata because the dendrites became confused in the tangle of other filled processes after diving down towards the somatic layer, therefore we did not attempt to classify the subtypes of cells from which we obtained our measurements. However, it is likely that most of the tufts that we imaged arose from mitral, rather than tufted mitral cells, because we imaged tufts several hundred micrometres long removed from the injection site, and as we attempted to follow apical dendrites back towards the somata we found almost all were >200 μm long before we lost track of the one we were following in the tangle of filled dendrites.

Glomeruli with two or more apical dendrites projecting into them were seen, indicating more than one filled set of tufts was located within. When more than one apical dendrite was seen entering a glomerulus, the corresponding tufts usually overlapped extensively so that 3-D reconstruction of the whole structure would be necessary in order to ascribe fluorescence changes to a particular tuft unambiguously. Examples, such as those shown in Figs 2i and 4 where spatially distinct regions of tufts could be followed back to different apical dendrites, were rare and in the absence of a means to determine the glomerular boundary we could not definitively say whether such examples comprised tufts in one or two glomeruli. A preliminary series of measurements indicated that the differences in time to onset and amplitude between branchlets in different regions of a glomerulus were small or not measurable. Therefore, we used measurement boxes that encompassed the majority of the filled structures in each glomerulus. It appears feasible and would be interesting to use two-photon microscopy in future studies to determine whether all the tufts within a glomerulus share similar odour sensitivities and similar $[\text{Ca}^{2+}]$ transient dynamics throughout their arborization, particularly at threshold odour concentrations, as some evidence suggests they might (Buonviso & Chaput, 1990).

Odour and nerve shock-evoked $[\text{Ca}^{2+}]$ transients

We measured the Ca^{2+} dynamics in MC apical tufts and distal portions of the apical dendrite with a temporal resolution ranging from 2 to 1000 ms. We tested the effect of odour stimulus strength on the $[\text{Ca}^{2+}]$ transient by increasing the puff duration over a range from short enough to elicit either a threshold LFP response or a small (e.g. 20% $\Delta F/F$) amplitude $[\text{Ca}^{2+}]$ transient, to long enough to elicit a maximal LFP and/or a maximal, i.e. no longer increasing, $[\text{Ca}^{2+}]$ transient (see Methods). A variety of characteristic responses to odour stimulation were seen in different tufts with respect to (1) the time to onset of the $[\text{Ca}^{2+}]$ increases (2), the rate of rise, (3) the duration of the transient, and (4) the sensitivity to ionotropic glutamate receptor blockade. These were compared with $[\text{Ca}^{2+}]$ transients resulting from electrical stimulation of the ON that produced the threshold to supramaximal LFP responses.

Time-course and amplitude of $[\text{Ca}^{2+}]$ transients

Odour applied to the nasal epithelium evoked a complex LFP response that lasted 1–2 s and was characterized by oscillations in the range of 7–15 Hz (e.g. Figs 3A and 4), as previously described (Delaney & Hall, 1996). In contrast, electrical stimulation of the ON evoked a brief stereotyped LFP response (Figs 3B and 6), followed by several seconds when spontaneous activity was suppressed (Delaney & Hall, 1996).

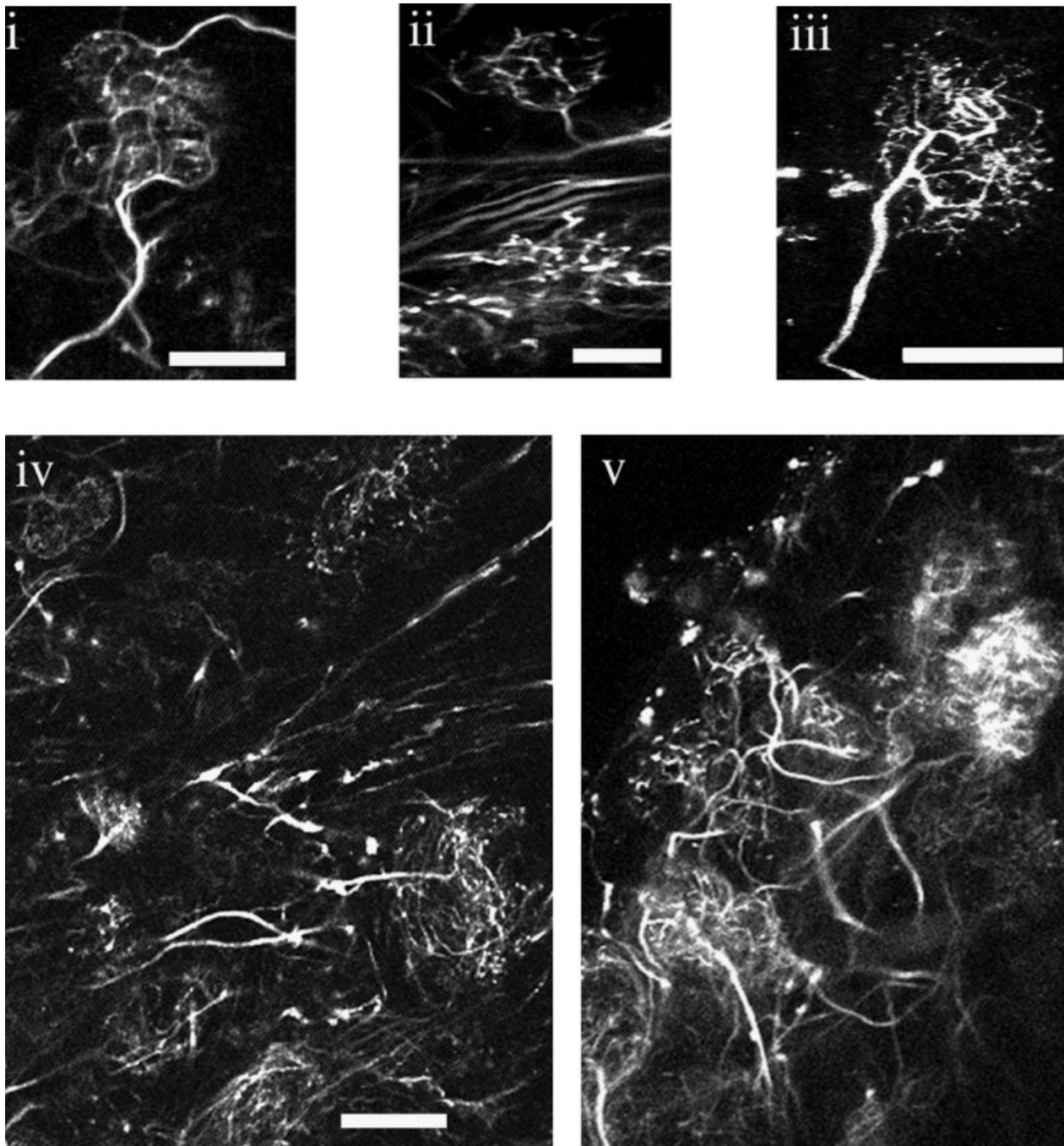


FIG. 2. Two-photon fluorescence images of mitral cell (MC) apical dendrites and dendritic tufts filled with dextran-conjugated Ca^{2+} -Green-1 in live intact olfactory bulb. All views are looking down on the ventral surface of the bulb or with the bulb slightly rotated to position the ventral-lateral face towards the lens. Panels (ii) and (iii) show tufts of single MC within the glomerular layer. Panel (i) shows an example of two filled tufts converging towards each other, possibly within the same glomerulus. Panels (iv) and (v) are wide-field images showing numerous filled tufts and apical dendrites within the glomerular layer. Image (iii) is a superimposed stack of z-scanned images, 90 μm of depth is compressed into a single image. Panels (i, ii and v) are 14-frame averages of single-plane scans. The location of the dye application was approximately 400 μm caudal, i.e. to the left-hand edge of (i–iii). Scale bars, 10 μm (i and ii), 40 μm (iii), 30 μm (iv and v). Rostral is towards the right in (iv) and the top in (v). In (v), the curvature of the bulb results in the appearance of an edge in the upper left.

$[\text{Ca}^{2+}]$ transients evoked by odours differed substantially from those evoked by electrical stimulation of the ON, in parallel with the differences in the electrical response of the OB (Fig. 3). Odour-evoked $[\text{Ca}^{2+}]$ transients were characterized by a prolonged rising phase, reaching their maximum approximately 1 s after their onset, regardless of the intensity or type of odour stimulus used. With strong

odour stimulation, maximal fractional fluorescence changes in the range of 50–100% were typical, i.e. 100–300 nM increases assuming resting $[\text{Ca}^{2+}]$ of 50 nM (see Methods). A few exceptional tufts reached nearly 150% $\Delta\text{F}/\text{F}$, suggesting $[\text{Ca}^{2+}]$ changes on the order of 700 nM. The long time to peak and nonexponential recovery of the transient indicate a sustained Ca^{2+} influx to the cytoplasm from

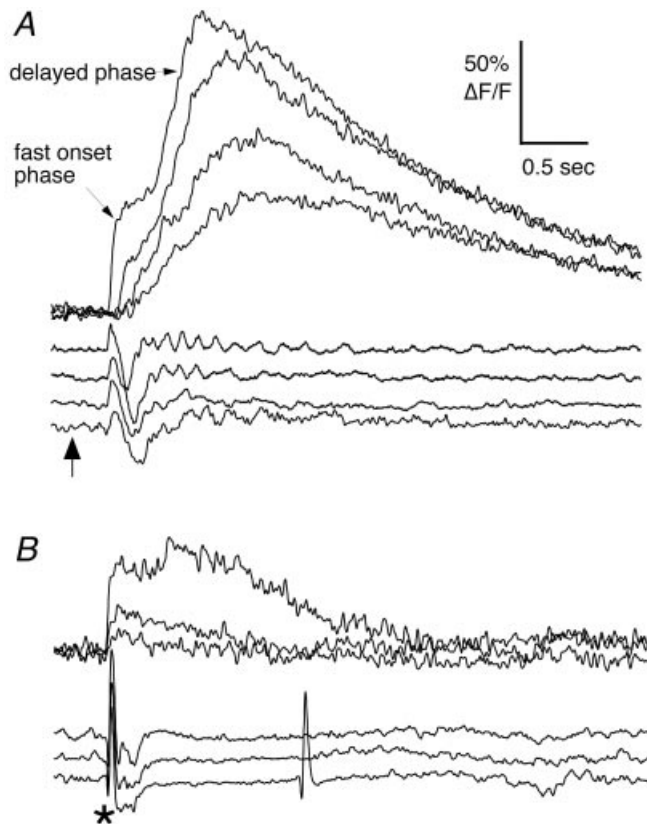


FIG. 3. (A) Large sustained Ca^{2+} transients result from odour stimulation of the olfactory epithelium. These data obtained from the tufts marked #3 in Fig. 4. Increasing odour puff duration (i.e. the intensity of odour stimulus, see Methods) increased the amplitude of the $[\text{Ca}^{2+}]$ transient, changed its shape and shortened the delay to the onset of the transient relative to the onset of the local field potential (LFP). Odour-evoked $[\text{Ca}^{2+}]$ transients (upper traces; smallest response to shortest puff, largest to longest puff) and LFP (lower set of traces, vertically offset for clarity, bottom is shortest puff, top is longest) to 10.5 kPa, 1: 1000 dilution amyl acetate puffs of 15, 17, 22 and 50 ms duration delivered (onset indicated by arrow) at intervals of about 2 min (order of delivery of puffs 50, 15, 17 then 22 ms). (B) Olfactory nerve (ON) shock evokes small, fast-onset, fast-decaying $[\text{Ca}^{2+}]$ transients without any change in delay with increasing stimulus intensity. Single ON shocks of 6, 7 and 10 V, as indicated by * below LFP traces. (Note in one trial a second 6-V stimulus was delivered 1.5 s after the first evoking a presynaptic volley but little synaptic response.) At the highest stimulus intensity, a small amplitude late phase is seen. Vertical scale is 50% $\Delta\text{F}/\text{F}$ for the all $[\text{Ca}^{2+}]$ transients as indicated and approximately 1 mV for the LFP, time-scale applies to all records.

extracellular space and/or from internally released Ca^{2+} stores. With more than 1–2 min between odour applications to permit full recovery of the LFP response, the peak of the fluorescence transient was repeatable to $\pm 20\%$ when the same stimulus was applied.

In tufts where the onset of the $[\text{Ca}^{2+}]$ transient was delayed more than 250 ms after the LFP onset, the transients showed a slow steady rise to a peak even with odour stimuli that evoked maximal LFP responses. When the onset of the $[\text{Ca}^{2+}]$ transient occurred shortly after the onset of the LFP response, it displayed a more complex rising phase (e.g. Figs 3A, 5 and 6). In these cases, an initial rapid rise in $[\text{Ca}^{2+}]$ was briefly interrupted and followed by a second, delayed, slower-rising phase. An initially rapid onset phase that could be distinctly separated from a later prolonged phase was most evident as stimulus intensity increased. This effect is particularly notable in Fig. 3A, which shows a series of high temporal resolution line scan measurements (data are from single line scans through middle of the

long axis of the tuft labelled #3 in Fig. 4). In tufts that did not show a dual phase onset to strong odour stimulation, the absence of an initial fast-rising component was better correlated with a longer delay to onset than with the amplitude.

As with odour-evoked $[\text{Ca}^{2+}]$ transients, the amplitude of the ON shock-evoked $\Delta[\text{Ca}^{2+}]$ was graded with the stimulation intensity. However, unlike odour stimulation, ON shock-evoked $[\text{Ca}^{2+}]$ transients were always characterized by an initial, rapidly rising phase. For low to moderate shock intensities, a peak of up to $\approx 25\%$ $\Delta\text{F}/\text{F}$ was reached within 10–30 ms of onset, followed by a relatively constant recovery (Figs 3B and 6). The amplitude of the initial fast-onset $[\text{Ca}^{2+}]$ transients produced by repeated presentations of the same intensity was always consistent within a narrow range, varying by $< 10\%$, provided a minute or more elapsed between shocks. An example of the repeatability of the $[\text{Ca}^{2+}]$ transient amplitude evoked by ON shocks repeated at long intervals is shown in the top three records in Fig. 6A (ON shocks indicated by *).

Prolonged elevation of $\Delta[\text{Ca}^{2+}]$, in the form of a broad, late peak, was only produced with high-intensity ON shock, in contrast with odour-evoked $[\text{Ca}^{2+}]$ transients that always had a late peak and long time-course. With electrical stimulation 0.8–2 times stronger than that which produced a maximal LFP, a second, sustained component developed in most tufts (Fig. 3B; also evident in third trace from top in Figs 6A and 12A). This delayed peak was similar in shape to the slow component of the odour-evoked $[\text{Ca}^{2+}]$ transient, usually starting to appear when stimulation intensity was strong enough that the initial fast-onset response was about 20% $\Delta\text{F}/\text{F}$. By increasing the ON shock intensity, the largest fast-onset, fast-decaying responses that we were able to elicit were 30–40% $\Delta\text{F}/\text{F}$. The largest amplitude slow components would attain their peak about 0.5 s later, and could add up to another 25% $\Delta\text{F}/\text{F}$ (estimated relative to the extrapolated recovery of the fast component) resulting in a second peak $\Delta\text{F}/\text{F}$ of about 40%. Electrolysis of theringer solution at the electrode tips limited the strength of the electrical stimulus we could deliver to the nerve to around 200–400 μA , 0.5 ms.

Time to onset of the $[\text{Ca}^{2+}]$ transient

Ninety percent (54/60) of tufts that responded to an odour puff had a $[\text{Ca}^{2+}]$ transient onset within 10–500 ms after the onset of the LFP response tested with a variety of odours at various puff durations. A few striking instances of delays of 1 s or greater were seen. For example, Fig. 4 shows four tufts measured simultaneously, where one tuft responds coincident with the onset of the LFP while the other three are delayed between 0.7 and 1.2 s. Onset delays in any given tuft were consistent with repeated presentations of the same odour stimulus, typically varying by $< 10\%$, thereby confirming that the wide range of onset delays we saw between tufts as we tested them individually in an experiment reflected real heterogeneity in responses to odours. Figures 5 and 9 show more examples where differences between onset times were verified when more than one tuft was measured simultaneously.

Increasing the odour stimulation consistently shortened the delay to onset. However, the extent to which onset delay was shortened depended upon whether the response to low-intensity stimuli was already brief (< 150 ms) or long. This effect is illustrated in Fig. 5 where onset delay is shortened in both tufts as puff duration is increased, with the tuft with the longer delay being most affected. Although the tuft with the later onset is more affected by increasing odour stimulation, its onset remains delayed relative to the other tuft over the range tested. Differences in onset delay between tufts and the systematic shortening with increasing intensity are unlikely to be caused by different Ca^{2+} -buffering in different tufts, as buffering can

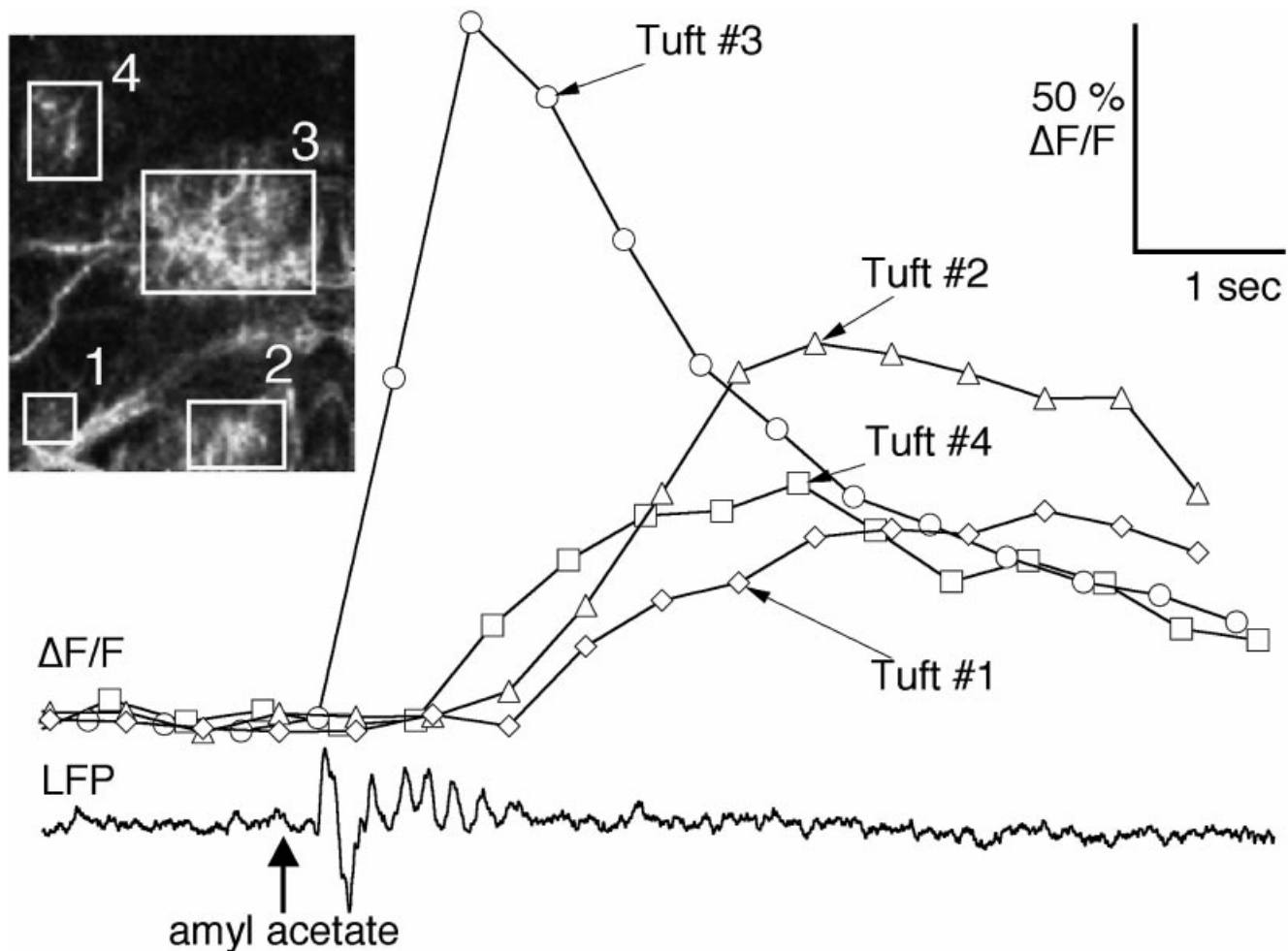


FIG. 4. Large differences in the time to onset of responses to odour stimulation in nearby tufts. In this large-field, low-temporal resolution scan, tufts in four glomeruli that responded to a 50-ms, 10.5-kPa puff (designated by vertical arrow on local field potential [LFP] trace) of amyl acetate are seen. Boxes on the inset image indicate the region from which fluorescence changes were measured for each tuft. Each image required 512 ms to acquire and the plotted data have been corrected for the scan delay between the top and bottom of the image based on the time of the line scanned through the middle of each measurement box. Lower trace is LFP.

suppress the amplitude of a $[Ca^{2+}]$ transient, but is unlikely to increase the delay to onset of $\Delta[Ca^{2+}]$ (Tank *et al.*, 1995).

With ON shock the onset of $[Ca^{2+}]$ transients always occurred within 0–10 ms after the onset of the LFP response (with TPLSM the single line scan rate limited our temporal resolution to 2 ms) and showed little or no shortening of latency with increasing intensity of stimulation (Fig. 3B). This is more evidence that the variable onsets of the $[Ca^{2+}]$ transient observed with odour stimulation are not the result of differences in Ca^{2+} buffering, and further supports the hypothesis that timing of ORN inputs and possibly local circuit processes are the primary factors determining the time to onset. We applied repetitive electrical stimuli to the ON to test whether the differences in $[Ca^{2+}]$ transients evoked by odour compared with an ON shock could be accounted for by the fact that odour stimulation activates repetitive firing on ORN afferents (Getchell & Shepherd, 1978). Repeated ON shocks at intervals less than 1–2 s produced a $[Ca^{2+}]$ transient to only the first stimulus ($n = 5$ tufts, three preparations), and the transient evoked by a second shock was attenuated by 50–100% for intervals up to 2 or 3 s (Fig. 6B). Thus, we found we could not mimic the repetitive firing of ORN afferents as occurs during odour stimulation to try to produce a sustained

$\Delta[Ca^{2+}]$ by stimulating short trains of low- or moderate-intensity ON shocks. This is not unexpected since substantial paired-pulse depression of the ON-evoked LFP in OB is a well-known phenomenon (Freeman, 1974; Jahr & Nicoll, 1982; Keller *et al.*, 1998). However, we could reliably evoke a large $[Ca^{2+}]$ transient with an odour stimulation even 0.5–0.75 s after a moderate to strong ON shock (Fig. 6; $n = 4$ different tufts in two preparations). A likely interpretation of these observations is that failure of the second of a pair of ON shocks to raise $[Ca^{2+}]$ was primarily the result of paired-pulse inhibition of the ORN terminals (Keller *et al.*, 1998). Partial suppression of the odour-activated responses by ON shock suggests that the odour activated some axons that were not previously stimulated by the ON shock and thus were spared from the full effect of the inhibition.

Pharmacology of odour and nerve shock-evoked $[Ca^{2+}]$ transients

Noting the prominent difference in the amplitude and time-course of odour-evoked compared with ON shock-evoked $[Ca^{2+}]$ transients, we tested for differences in the sensitivity of the $[Ca^{2+}]$ transients to blockade of NMDA and AMPA receptors. Previous studies of the

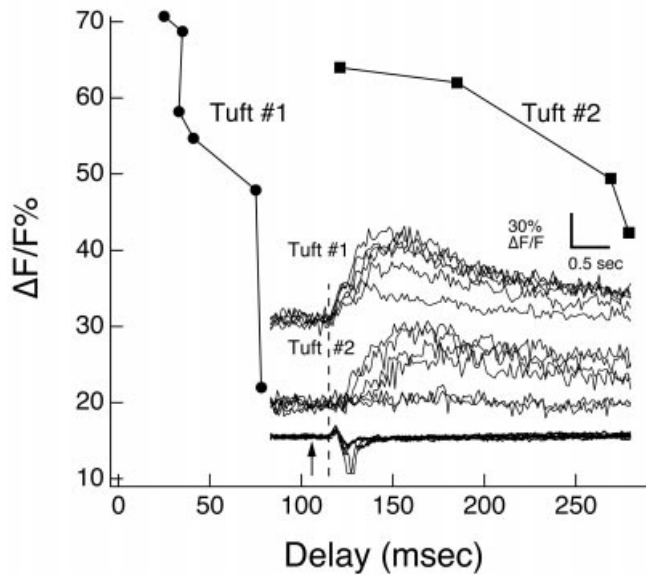


FIG. 5. Differences in delay to onset between different tufts persist as odour intensity is increased. Graph shows fluorescence change vs. delay to onset for the two tufts with increasing puff duration. The inset shows $[\text{Ca}^{2+}]$ transients in two tufts separated by about $75 \mu\text{m}$ in the same field of view from which data for the graph were obtained. Note no response was elicited in tuft 2 to the two lowest intensity stimuli. Measurement boxes of 12×12 pixels were positioned over each tuft, frame interval was 32 ms. Stimuli were 1: 1000 v/v *n*-butanol puffs (17, 19, 29, 31, 37 and 43 ms, onset indicated by arrow). Lower traces are the local field potentials (LFPs). The onset of the odour-evoked LFP response used as the timing reference is indicated by the dashed vertical line.

sensory synaptic potential in MCs revealed that the amplitude of the AMPA-R- and NMDA-R-mediated components of the excitatory postsynaptic potential produced by electrical stimulation of afferents in mammalian bulb slices were about equal (Berkowicz *et al.*, 1994), with the NMDA-sensitive component being longer lasting.

The efficacy of AMPA-R vs. NMDA-R blockers depended upon the strength of the stimulus and whether odour or ON shock was used (Figs 7 and 8). Weak ON shock-evoked responses (i.e. submaximal LFP response and $[\text{Ca}^{2+}]$ transients with only a rapid onset, fast-decaying time-course) were almost entirely blocked by $10 \mu\text{M}$ CNQX (14% \pm 12% of control amplitude; $P < 0.0005$; $n = 8$), but virtually unaffected ($113 \pm 16\%$ of control, mean \pm SEM, $n = 6$ preparations) by saturating concentrations of AP5 (100–150 μM). In contrast, when stronger ON shocks were delivered that produced a distinct late peaking component in the $[\text{Ca}^{2+}]$ transient, CNQX blocked a part of the initial phase of the transient leaving a long-lasting phase that was subsequently blocked by AP5 (Fig. 7C, $n = 5$).

In contrast to ON shock, odour-evoked responses to all intensities of stimulation were significantly blocked by AP5, but not by CNQX (Fig. 8). In fact, strikingly, in 9/11 cases CNQX increased the peak of the odour-evoked fluorescence transient for an overall average of $134 \pm 30\%$ of control ($P < 0.025$; $n = 11$). AP5 alone reduced the peak of the odour-evoked fluorescence transient in all cases to an average of $46 \pm 16\%$ of control ($P < 0.0025$; $n = 7$). Because the amplitude of odour-evoked fluorescence transients is normally high enough to partially saturate the indicator, these percentage reductions in fluorescence correspond to even larger reductions in $\Delta[\text{Ca}^{2+}]$.

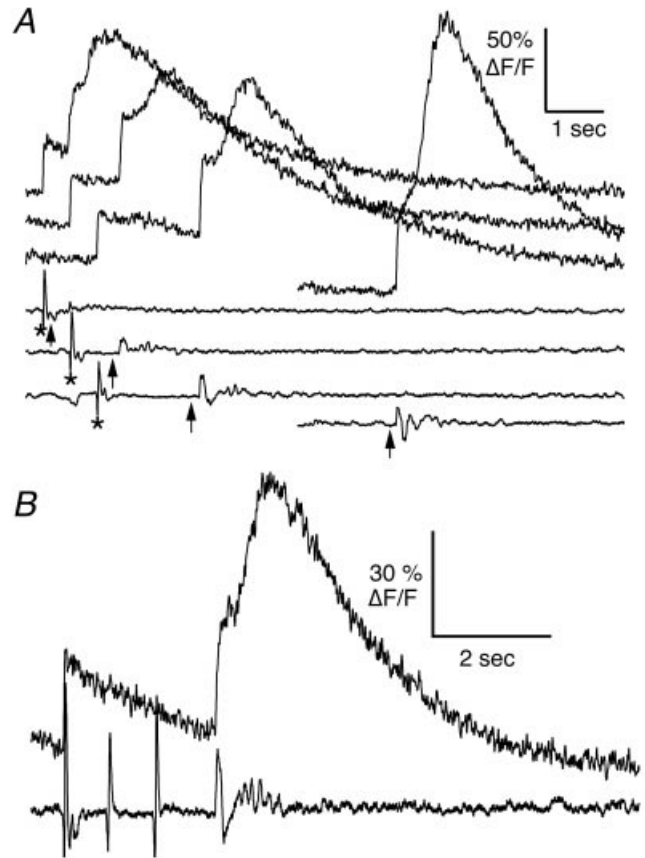


FIG. 6. (A) Suppression of the odour-evoked local field potential (LFP) and $[\text{Ca}^{2+}]$ transient follows olfactory nerve (ON) shock. Upper set of traces are fluorescence changes, lower set of traces are corresponding LFPs. An ON shock (*) evokes a typical fast-rising, rapidly recovering $[\text{Ca}^{2+}]$ transient. Odour-evoked (arrow) LFP and $[\text{Ca}^{2+}]$ transients which follow within a few seconds after an ON shock (top three traces) are smaller than an odour-stimulus without preceding shock (bottom pair of traces, offset to right for clarity). At shorter intervals, suppression of the odour-evoked LFP increases and is almost complete, but the reduction in the odour-evoked $[\text{Ca}^{2+}]$ transient is more sensitive to preceding ON shock than the fast component in this example. (B) Multiple ON shocks do not suppress odour-evoked $[\text{Ca}^{2+}]$ transients more than single shocks (same tuft as in part A). Only the first of three successive ON shocks delivered at intervals of 0.75 s produces a $[\text{Ca}^{2+}]$ transient in the tuft (first three arrows). An odour puff (*) delivered 0.75 s after the third ON shock produces a robust local LFP with oscillations and a $[\text{Ca}^{2+}]$ transient composed of fast and slow components. Suppression by three ON shocks is similar to that of single ON shock with an interval of 75–150 ms between shock and odour delivery (see part A).

Differential responses to different odours

By alternating stimulation with two odours, we tested for differential sensitivity among tufts. Dramatically different response profiles could be observed with tufts located in glomeruli separated by 50–75 μm (Fig. 9). The most dramatic examples of discrimination were seen when tufts in adjacent glomeruli responded to only one of the odours regardless of the intensity of stimulation. In other cases, one odour would be specific to one tuft while the other activated both tufts, although not necessarily equally. As mentioned previously, we found that there could be differences in the time-course and latency to onset of the response, even if the amplitudes were very similar (Figs 4, 5 and 9B). This is a further argument against a role for Ca^{2+} buffering

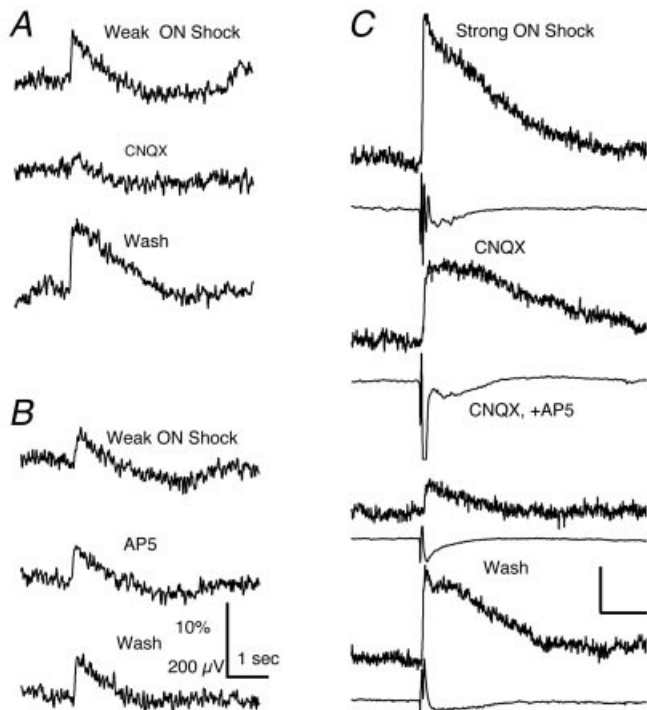


FIG. 7. (A and B) $[Ca^{2+}]$ transients evoked by weak olfactory nerve (ON) shock are blocked by $10 \mu M$ CNQX but not affected by $100 \mu M$ AP5. Scale bars are vertical, $10\% \Delta F/F$, $200 \mu V$ and horizontal $0.5 s$. (C) $[Ca^{2+}]$ transients evoked by strong ON shock contain both a CNQX- and a AP5-sensitive component, the greater portion of which is AP5-sensitive. Scales are 10% , $200 \mu V$ and $1 s$ for all.

by the indicator as a cause for variation in onset delays observed in different tufts when the same odour was used to stimulate the nose.

Feedback inhibition from stimulation of the lateral olfactory tract suppresses $[Ca^{2+}]$ transients in tufts

We explored the effect of synaptic inhibition of MCs by intrinsic OB circuitry on odour-evoked $[Ca^{2+}]$ transients using electrical stimulation of the LOT to evoke feedback inhibitory postsynaptic potentials (IPSPs) in MCs. Localized electrical stimulation of the LOT at the dorsolateral edge of the posterior bulb/rostral telencephalon activates MCs antidromically (Jiang & Holley, 1992b), resulting in a GABAergic feedback IPSP (Jahr & Nicoll, 1982; Chen *et al.*, 1997; Fig. 10). In frogs, the projection of the LOT to the cortex is less discrete than in mammals and some MC axons leave the bulb via a medial olfactory tract along the boundary between left and right hemibulbs. Using an electrode placement similar to ours, Jiang & Holley (1992b) found that up to 50% of the MCs they sampled intracellularly *in vivo* were activated antidromically by stimulation of the LOT, while all MCs show a delayed IPSP due to the divergence of GC inhibitory synapses. We found that LOT shocks led to brief $[Ca^{2+}]$ transients, of the order of 5–10% $\Delta F/F$ in somata and secondary dendrites of MCs in 3/3 preparations that we tested, which is consistent with observations from slices of rat OB (Isaacson & Strowbridge, 1998). However, we did not see stimulus-locked transients in any of the 17 apical tufts in six different bulbs that we examined while stimulating the LOT in this study.

First, we looked at the effect of LOT shocks on spontaneous $[Ca^{2+}]$ transients. A small fraction (<10%) of tufts exhibited spontaneous (10–20% $\Delta F/F$), fast-rising Ca^{2+} transients (Fig. 10A). These transi-

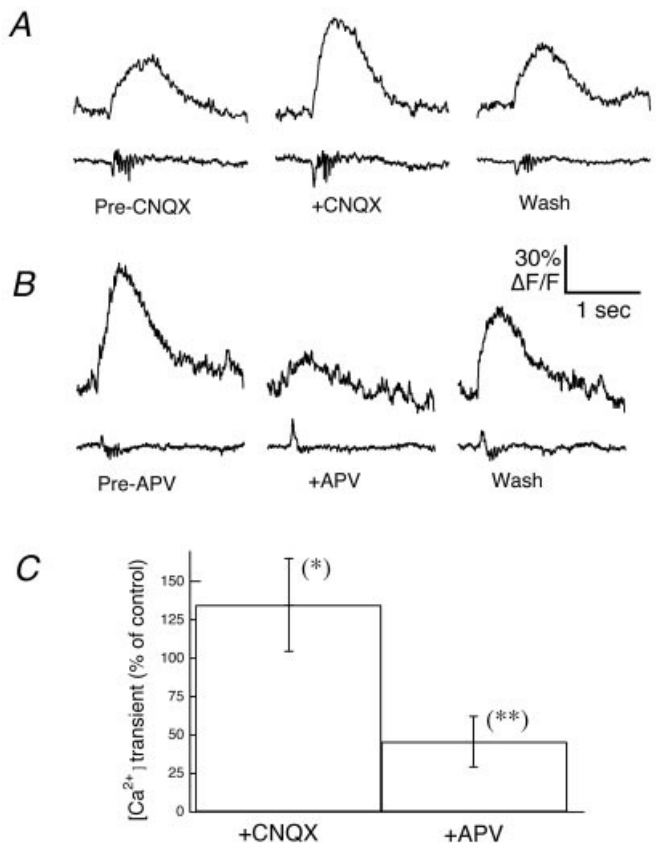


FIG. 8. (A) AMPA-R blockade by $10 \mu M$ CNQX reversibly increases the odour-evoked $[Ca^{2+}]$ transient. (B) NMDA-R blockade with $150 \mu M$ AP5 strongly suppresses the odour-evoked $[Ca^{2+}]$ transient. Traces are representative fluorescence and local field potential records while bars (C) summarize data for CNQX ($n = 11$) and for AP5 ($n = 7$). Vertical scale is $30\% \Delta F/F$, $600 \mu V$.

ents peaked within 50–100 ms and recovered monotonically with a time constant of roughly 0.5 s. The long time to peak may suggest they the result from sustained Ca^{2+} -dependent action potentials. Short trains of antidromic LOT shocks suppressed spontaneous activity, without inducing detectable $[Ca^{2+}]$ transients themselves ($n = 4/4$ tufts tested this way). We do not know whether these cells that showed high rates of spontaneous transients were in a physiologically compromised state, or whether they represent a subclass of MC in which spontaneous dendritic spikes are common (Mori *et al.*, 1982) or cells for which antidromic invasion of action potentials from the soma are particularly effective for elevating $[Ca^{2+}]$. Note, however, that there is no evidence for a LOT-activated, antidromic action potential-mediated $\Delta[Ca^{2+}]$ in the records shown in Fig. 10A.

We next examined the effect of LOT-induced feedback inhibition on odour-evoked $[Ca^{2+}]$ transients. Consistent with a strong GABAergic feedback IPSP to MCs, we found that trains of LOT shocks (3–6 stimuli) were highly effective in blocking or reducing odour-evoked Ca^{2+} transients (Fig. 11). Properly timed trains of 5–6 LOT shocks reduced large (>50% $\Delta F/F$ to begin with), early onset odour-evoked fluorescence transients by 60–75% (Fig. 11, $68 \pm 8\%$, mean \pm SD, $n = 8$ tufts) and completely eliminated weaker, delayed-onset $[Ca^{2+}]$ transients ($n = 2$, data not shown). Due to partial dye saturation, these reductions in $\Delta F/F$ correspond to even greater reduction of $\Delta[Ca^{2+}]$. Suppression of odour-evoked $\Delta[Ca^{2+}]$ by LOT shock was always repeatable, as shown directly in Fig. 11B, and

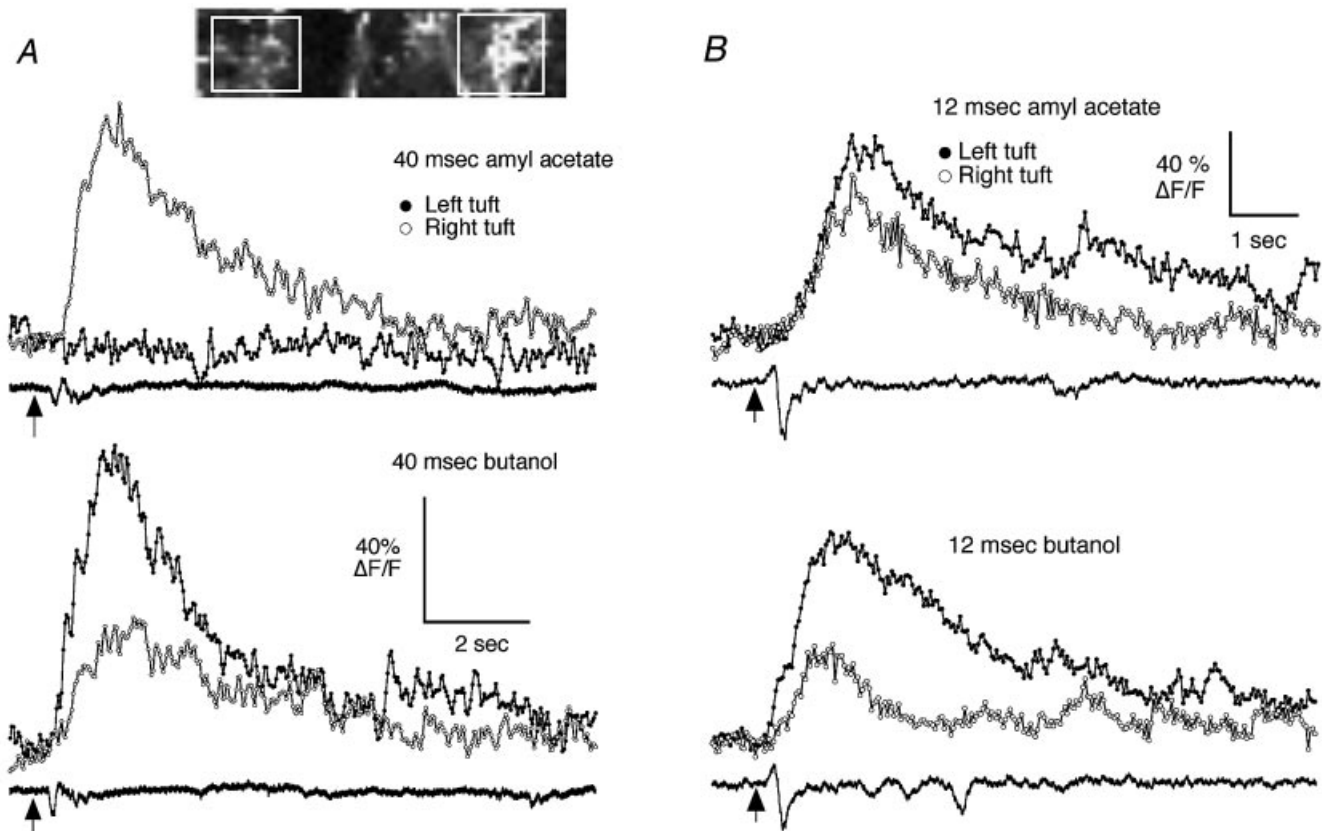


FIG. 9. (A) Marked differences in the responses to different odours are often seen in tufts that were located near each other. Boxes over the image indicate the locations from which fluorescence measurements were made from tufts located about 50 μm apart. In the upper panel the left tuft shows no response to amyl acetate while in the lower panel this same tuft shows a large rapid onset response to butanol. In contrast the right tuft responds to both odours, but less robustly to butanol. (B) In other instances, nearby tufts responded to both odours tested but with different time-courses and magnitude. Data in B are from a pair of adjacent tufts in a different preparation from those in A. In the upper panel, the left tuft responded to amyl acetate with a slowly rising large response. In the lower panel, this same tuft shows a two-component response with a more rapid onset. The right tuft responds to both odours with a predominantly slow time-course that is smaller for butanol than for amyl acetate.

reversible. The absence of suppression by a single LOT stimulus (illustrated in Fig. 11B) was consistent with observations of Mori *et al.* (1984) who studied the effect of LOT shock upon ON shock-evoked excitatory postsynaptic potential (EPSP) in MCs (Mori *et al.* did not test the effects of trains of LOT shocks). Their observations indicated that summation of the IPSP was required, perhaps to provide inhibition of a sustained duration to oppose the sustained excitation of the odour stimulation.

The timing of the LOT stimuli relative to the onset of odour responses was important for producing maximal suppression (Fig. 11C). We found the block of the odour-evoked Ca^{2+} transients was most effective when the onset of LOT stimulation was approximately coincident with delivery of the odour. Note that by starting the LOT shock train when the odour was applied, the second or third LOT stimulus in the train coincided with the time when the odour response would begin in the bulb because there is normally at least a 200 ms delay from the onset of odour stimulation at the nose to the initiation of $[\text{Ca}^{2+}]$ transients while the delay between LOT stimulation and the LFP response is 10 ms or less. The blocking of the odour-evoked Ca^{2+} response was weaker ($n = 2$ tufts) when the train of LOT shocks preceded the odour puff by >500 ms, i.e. the last shock occurred about 100–200 ms before the onset of the odour-evoked response (Fig. 11C). This suggests a rapid decay for the inhibitory effect

of LOT stimulation as would be expected if it was mediated predominantly by GABA_A receptors.

The time-course of the hyperpolarization in a MC produced by a single LOT shock and for a train of stimuli is shown in Fig. 10B and C. Failure of the later stimuli in the train to evoke a full amplitude action potential, as shown in this example, was observed in MCs from 3/3 other preparations. So, although we did not simultaneously image tufts and measure MC electrophysiology, we believe this is likely to fairly represent the conditions of our optical recording experiments (see also Jahr & Nicoll, 1982). We also found that delivery of several LOT stimuli starting within 0.5 s after the onset of the odour-evoked Ca^{2+} response could still substantially reduce the $[\text{Ca}^{2+}]$ transient ($n = 3/5$ tufts in two preparations; e.g. Fig. 11C).

Experiments to investigate the role played by GABA_A receptors in shaping the time-course of fluorescence transients and in mediating LOT-induced inhibition were difficult to perform because of the tendency for the preparation to become hyperexcitable in the presence of GABA_A blockade. Figure 12 summarizes our observations of the effects of 10 μM bicuculline on ON shock and odour-evoked fluorescence transients. Bicuculline reliably increased the amplitude of both odour and ON shock-evoked transients, and eliminated evidence for a pause in the rising phase for early onset responses, while not reliably extending the duration of the fluorescence transient (Fig. 12A and B). These data support the hypothesis

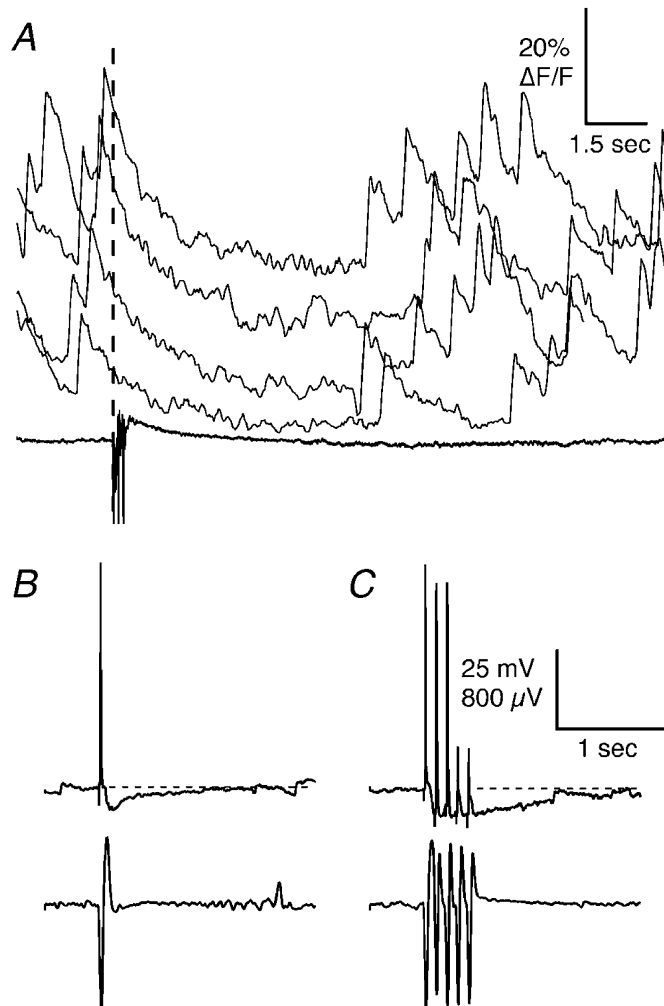


FIG. 10. (A) Trains of lateral olfactory tract (LOT) stimuli reduce the frequency of spontaneous $[Ca^{2+}]$ transients. In tufts showing regular spontaneous transients, LOT stimulation was effective for transiently suppressing these transients in a nongraded manner. Note that the LOT stimuli (a train of three at 10 Hz in this example) did not evoke transients themselves. Vertical dashed line indicates onset of LOT stimulus trains. Four successive responses to LOT stimulation are shown vertically offset for clarity. Interval between each train of LOT stimuli was 30 s. (B and C) Whole-cell recording from a mitral cell during delivery of a single (B) or a train of five LOT shocks at 10 Hz (C). Note the summing and longer-lasting inhibitory postsynaptic potential (IPSP) that follows the train of antidromic action potentials with the repetitive stimulation and the failure of antidromic action potentials in the recorded cell to reach threshold at the peak of the IPSP. Panels (B,C) provided by B. Hall.

that rapid feedback inhibition shapes the early phases of the response to odours and limits expression of the excitatory input from olfactory afferents for both ON shock and odour stimuli. In Fig. 12C we present representative data from one of three experiments in which the dependence of the LOT-induced inhibition of odour-evoked fluorescence transients on $GABA_A$ receptor activity was tested. In two experiments, data like those shown were obtained, namely showing that bicuculline blocked the LOT-induced inhibition of the odour-evoked fluorescence transient. In another preparation, no effect of the LOT stimulus was observed for reasons that are unclear, but this is similar to the pattern in other experiments where transients in a small number of preparations or tufts failed to respond to LOT stimulation

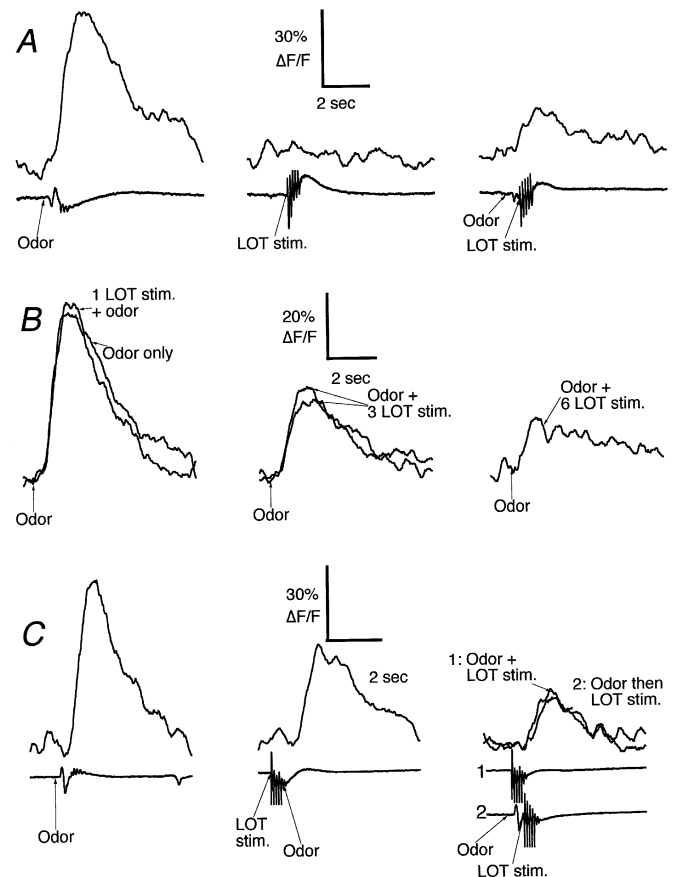


FIG. 11. Suppression of odour-evoked $[Ca^{2+}]$ transients by stimulation of the lateral olfactory tract (LOT). Results from three different preparations are shown. (A) Left panel: response to odour puff alone, top is fluorescence, bottom is local field potential (LFP). Middle panel: a train of five LOT shocks at 10 Hz without odour does not elevate $[Ca^{2+}]$ in the tuft. Right panel: the same train of LOT shocks reduces the odour-evoked $\Delta F/F$ transient by 73%. In this example, the first LOT stimulus in the train was delivered so as to arrive at the bulb about 400 ms after the onset of the odour-evoked LFP. (B) Increasing the number of LOT shocks in a train increases suppression. First stimulus in a 10-Hz LOT shock train was delivered coincident with an odour puff (indicated by arrow), i.e. about 200 ms before the onset of the odour-evoked LFP. Left panel: odour alone and odour plus one LOT stimulus as indicated. Middle panel: odour plus three LOT stimuli. Right panel: odour plus six LOT stimuli. Fluorescence traces shown grouped by increasing effect of LOT stimulus. The actual order of presentation was odour plus three, six, zero and then three LOT stimuli in the train. Each trial separated by 2 min. The effect of three shocks was tested twice to demonstrate the repeatability of the effect. (C) Left panel: odour alone. Middle panel: five LOT stimuli at 10 Hz delivered starting 0.5 s prior to an odour puff suppresses the odour-evoked $[Ca^{2+}]$ transient (compare left and middle panels). Right panel: LOT shocks delivered coincident with an odour puff (traces labelled 1) or 0.5 s after the puff (traces labelled 2) are equally effective for suppressing the odour-evoked $[Ca^{2+}]$ transient and in this case more effective than LOT stimulation delivered 0.5 s before the odour. Vertical scale is approximately 1 mV for LFP records in A and B.

Discussion

By measuring the $[Ca^{2+}]$ in glomerular tufts, we are beginning to understand the separate computational dynamics in these most distal dendritic compartments of mitral cells (MC). It is clear from our data that cytoplasmic $[Ca^{2+}]$ is increased by several hundred nM for more than 1 s in tufts responsive to a particular odour. Given the magnitude and duration of the odour-evoked $[Ca^{2+}]$ increase, it is probable that it

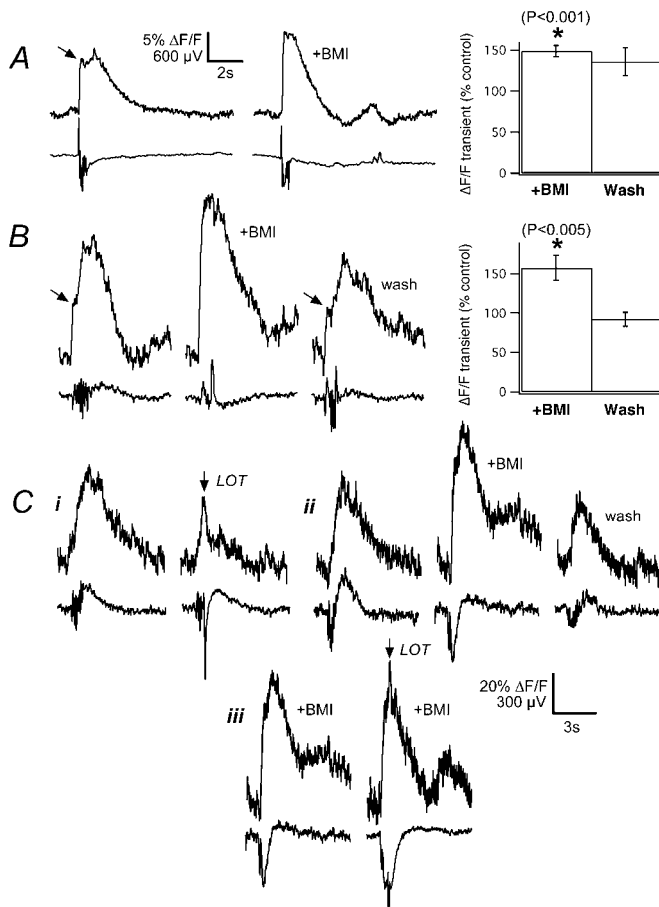


FIG. 12. Effects of GABA_A receptor blockade on the time-course of $[\text{Ca}^{2+}]$ transients and efficacy of lateral olfactory tract (LOT)-induced inhibition. (A) Upper traces are fluorescence measurements from a tuft in response to a strong intensity electrical stimulation of the olfactory nerve (ON) (three stimuli at 33 Hz, 0.5 ms 15 V), lower traces are corresponding local field potential (LFP) recordings. Arrow points to the dual-phase response characteristic of the strongest ON stimuli that consists of a fast-onset $[\text{Ca}^{2+}]$ increase then a brief pause in the rise that is followed by a sustained $[\text{Ca}^{2+}]$ transient. The left pair of traces are control, the right pair are responses in the presence of $10 \mu\text{M}$ bicuculline. Bar graph summarizes the mean \pm SEM change in peak amplitude of the fluorescence transient from six cells in five preparations. The * indicates statistical difference between bicuculline treatment ($149 \pm 6.5\%$) and control at $P < 0.001$. (B) Upper traces are fluorescence measurements from a tuft that responded to odour stimulation with a biphasic response. Arrows indicate the brief pause in the rising phase following the rapid onset fluorescence change that was seen prior to and after washing off $10 \mu\text{M}$ bicuculline, but not during bicuculline. Bicuculline reliably eliminated the pause in the rising phase of the fluorescence transient and increased the amplitude of the peak response, as summarized in the bar graph to the right (17 cells, 13 preps for control, 16 cells for washout, bicuculline $158 \pm 16\%$ of control). (C) Traces are responses to 100 ms, 1.6 kPa puff of 1: 1000 *n*-butanol in the same preparation. (i) Left pair control, right pair with addition of a train of four LOT shocks delivered to arrive shortly after the onset of the odour-evoked response. The train of LOT shocks truncates the odour-evoked fluorescence transient (see also Fig. 11). (ii) Addition of $10 \mu\text{M}$ bicuculline enhances the odour-evoked fluorescence transient in a reversible manner, and (iii) blocks the LOT-mediated inhibition in this cell.

could trigger biochemical processes, such as transmitter release or other synaptic plasticity phenomena in the tuft, and is thus a potential cellular variable in olfactory processing. For example, the sustained cytoplasmic $[\text{Ca}^{2+}]$ increase evoked by odour stimulation could in principle facilitate the transmitter-releasing capacity of a brief action

potential-mediated Ca^{2+} influx from back-propagating or dendritically generated spikes if these are present in frog as they are in mammal. The synaptically evoked increased $[\text{Ca}^{2+}]$ could be releasing transmitter directly, given recent data showing that influx through NMDA channels can support release from dendrites under certain conditions (Chen *et al.*, 2000; Halabisky *et al.*, 2000), and well-known examples of graded transmitter release in retinal neurons and invertebrate neural processes (e.g. Graubard *et al.*, 1980; Laurent, 1993). The temporal, pharmacological, spatial and amplitude differences between odour-evoked and ON shock-evoked $[\text{Ca}^{2+}]$ transients that we have observed indicate the importance of using odour stimulation when possible to try to understand the dynamic function of the OB circuitry in determining the neural output to higher centres.

Ca^{2+} transients in mitral cell tufts evoked by odours and olfactory nerve shock: delay to onset

Odour-evoked responses were larger and more variable in their onset and time-course than those elicited by electrical shocks to the ON. Correlated with this difference in $[\text{Ca}^{2+}]$ transients, odour stimulation and ON shock differ in their ability to elicit oscillatory activity within the bulb; single stimuli or trains of ON shocks will not induce sustained oscillatory responses in healthy preparations while odours readily activate large-scale oscillations in the bulb LFP (Delaney & Hall, 1996). Sustained odour-evoked excitatory synaptic input to the bulb circuitry was an essential feature of one of the original models for the generation of odour-evoked oscillations (Rall & Shepherd, 1968). From our data, a sustained drive to the MC population in the bulb can be inferred from the dispersion of onset delays between tufts in different glomeruli (onsets between glomeruli are spread out over 10–1000 ms or more), and the long duration (1 s or more to peak) for $[\text{Ca}^{2+}]$ transients produced by stimulation of the nose with odours.

The wide variation in time to onset of $[\text{Ca}^{2+}]$ transients that we observed between tufts is similar to the range of delays to onset of firing for ORNs following odour application (Getchell & Shepherd, 1978; Getchell, 1986). The tendency for shorter delay to onset with increased odour intensity, particularly in tufts that showed no response or long delays to lower intensity stimuli, is consistent with the observation that increasing stimulus strength shortens the time to onset of ORN action potentials (Getchell & Shepherd, 1978; Trotter & Døving, 1996; Duchamp-Viret *et al.*, 2000). The difference in the time to $[\text{Ca}^{2+}]$ transient onset and the effects of increasing odour strength that we saw between tufts in different glomeruli with application of the same odour is also consistent with sets of similarly tuned ORNs that converge onto different glomeruli. Although all our observations regarding the onset of the $[\text{Ca}^{2+}]$ transient in tufts might be parsimoniously explained by differences in timing of afferent firing, inhibitory synaptic inputs could, in principle, further control the onset of Ca^{2+} influx. Given that synaptic inhibition can suppress Ca^{2+} influx when properly timed with odour stimulation and the fact that afferents can fire repetitively for a second or more in response to odour stimulation, it is possible that synaptic inhibition could delay the onset of the Ca^{2+} influx as well.

Ca^{2+} transients in mitral cell tufts evoked by odours and olfactory nerve shock: time-course

It is more difficult to account for the time-course of the odour-evoked $[\text{Ca}^{2+}]$ transients and for the effects of increasing stimulus strength by extrapolating from the probable firing patterns of presynaptic afferents. ORN firing pattern in response to high odourant concentration usually consists of an initial high-frequency burst followed by lower sustained rates of firing (Getchell & Shepherd, 1978; Duchamp-Viret *et al.*, 1990, 2000). This would not account for the

pause in the rising phase of the transient seen with short-onset, large-amplitude responses. A simpler possibility is that inhibitory feedback transiently suppresses the Ca^{2+} influx driven by a single, fast-onset and persistent drive, 'sculpting' it to look like separate events. In this model, either sustained release of transmitter from maintained ORN firing, and/or a long-lasting excitatory postsynaptic current could provide the drive that feedback inhibition then transiently interrupts and/or suppresses. Data presented in Fig. 12 support this hypothesis. Alternatively, or in addition, the second late, large $\Delta[\text{Ca}^{2+}]$ increase may have a component driven by release from internal stores (Emptage *et al.*, 1999), or an accumulation of glutamate (Isaacson, 1999; Carlson *et al.*, 2000) or potassium (Jahr & Nicoll, 1981) in the restricted extracellular space in the glomerulus may play a role. These latter hypotheses remain to be explored.

Is the long-lasting, odour-evoked $[\text{Ca}^{2+}]$ transient only the result of sustained firing of presynaptic afferents or is there an intrinsically long-lasting component to the EPSP? Olfactory nerve shock stimulates a synchronous volley of action potentials with little temporal dispersion of synaptic inputs because ORN axons have similar conduction velocities (Getchell, 1986). Excitation of MCs by ON shock is rapidly followed by long-lasting inhibition, predominantly due to a GABA_A IPSP. When GABA_A inhibition is blocked in isolated turtle bulb (Nowycky *et al.*, 1981) and in mammalian OB slices, where the orientation of the cut can reduce the strength of GC inhibitory inputs (Berkowicz *et al.*, 1994; Nickell *et al.*, 1996), a long-lasting depolarization of MCs is seen in response to a single ON shock. Although we saw smaller $[\text{Ca}^{2+}]$ transients and had difficulty eliciting a sustained increase in $[\text{Ca}^{2+}]$ with ON shock, when we managed to elicit a late, sustained $[\text{Ca}^{2+}]$ influx with high-intensity ON shock, it was substantially blocked by AP5, like the odour-evoked response. Therefore, we conclude that strong, but not weak, ON shock provides sustained excitation of MCs, primarily through NMDA-R activation. We propose that this NMDA-R component is usually masked or suppressed by inhibition, and the shorter duration and smaller amplitude of the ON shock-evoked $[\text{Ca}^{2+}]$ transient is due to both the synchronous activation of feedback inhibitory inputs and the absence of a repetitive train of sensory afferent action potentials.

When ON stimulation is sufficiently strong to initiate a late peak in the $[\text{Ca}^{2+}]$ transient, the peak occurs with approximately the same delay as the late peak of an odour-evoked response. This also suggests that temporally distributed, repetitive firing of ORNs is not the only determinant of the late time to peak of the slow component of odour-evoked $[\text{Ca}^{2+}]$ transients. Persistence of glutamate released by activation of many convergent ORN terminals and/or the MC tufts themselves within the closed space of the glomerulus might sustain activation of NMDA-R (Isaacson, 1999; Matsui *et al.*, 1999).

Recently, long-lasting depolarization of mitral cells in rat OB slices has been reported in response to afferent fibre stimulation (Carlson *et al.*, 2000). The time-course of these responses is strikingly similar to our odour-evoked Ca^{2+} transients and transients evoked by our strongest ON shocks. These responses in rat bulb slices differ from our odour-evoked long-lasting $[\text{Ca}^{2+}]$ transients in that they are not dependent on activation of NMDA receptors. The long-lasting depolarizations reported by Carlson *et al.* do, however, have a significant NMDA component that enhances their amplitude and duration. It seems likely, therefore, that there is some component of our long-lasting $[\text{Ca}^{2+}]$ transients that results from excitatory interactions among the apical dendrites of MCs. The weak dependence of our odour-evoked $[\text{Ca}^{2+}]$ transients upon AMPA receptors and the prominence of NMDA-dependent responses in the presence of physiological levels of Mg^{2+} plus AMPA blockade may reflect a weak voltage dependence for NMDA receptors in frog distal

dendrites and/or the effect of persistent release of glutamate by trains of ORNs activated by odours.

Pharmacology of odour-evoked Ca^{2+} transients

AMPA-R blockade usually increased the odour-evoked $[\text{Ca}^{2+}]$ influx suggesting that for odour stimulation NMDA-Rs may be more important relative to AMPA-Rs for exciting MCs than previous studies based upon ON shock activation suggested. We hypothesize that this is probably due to blockade of AMPA-R-mediated synaptic excitation of inhibitory PG neurons by ORN that is present spontaneously (Rosspars *et al.*, 1994), or during sustained excitation by an odour. Our own whole-cell recordings (Dieudonne *et al.*, 2000) and those of (Bardoni *et al.*, 1996) indicate that AMPA-R blockade eliminates virtually all ON shock-evoked excitatory input to PG neurons. Block of PG excitation would both disinhibit MC and reduce presynaptic inhibition of ORN terminals (Keller *et al.*, 1998) that otherwise would be expected to develop during sustained, odour-evoked ORN firing. Because NMDA-R activation appears to be required for the majority of the sustained Ca^{2+} influx to MC during odour stimulation (or strong ON shock), AMPA-R blockade can shift the balance of odour-evoked synaptic excitation and inhibition towards excitation. This suggests that during odour stimulation unblocking of NMDA-R by AMPA-R-mediated depolarization is not required for frog mitral cells, and experiments are underway to examine this hypothesis directly (Davison & Delaney, 2000).

Inhibition of Ca^{2+} transients by lateral olfactory tract shock

Antidromic activation of MCs by LOT stimulation was an effective way to suppress odour-evoked $[\text{Ca}^{2+}]$ transients. At this time we believe our data suggest that the reduction in the odour-evoked $[\text{Ca}^{2+}]$ transient by LOT stimulation is due primarily to the GC–MC rather than the PG–MC synapses. Our placement of the bipolar stimulating electrode on the dorsolateral face of the rostral telencephalon should avoid stimulating centrifugal fibres from telencephalic and brainstem nuclei that might project to the glomerular layer, so this possibility can be discounted. Transmitter release from the tuft requires elevated $[\text{Ca}^{2+}]$, but we saw no evidence of LOT-evoked $[\text{Ca}^{2+}]$ transients (Figs 10–12).

The absence of antidromic action potential-dependent $[\text{Ca}^{2+}]$ transients in response to LOT stimulation may simply reflect that these transients were too small to resolve routinely under our experimental conditions. Especially during the odour-evoked $[\text{Ca}^{2+}]$ transient ($> 100\% \Delta F/F$), indicator saturation would greatly reduce the ability to discern $\Delta F/F$ transients corresponding to individual action potentials. Although back-propagation of the action potential into the distal dendrite is electrically robust under normal conditions in mammals *in vitro* (Bischofberger & Jonas, 1997; Chen *et al.*, 1997; Isaacson & Strowbridge, 1998) and *in vivo* (Charpak *et al.*, 2001), there is currently little direct evidence to indicate that antidromic action potentials always release large amounts of neurotransmitter. Freeman (1974) reported that LOT stimulation did not activate units in the glomerular layer of anaesthetized rabbit (see also Wellis & Scott, 1990). Antidromic MC action potentials activated via the medial olfactory tract in frog OB slices produced EPSPs in only 5% of recorded PG neurons (Bardoni *et al.*, 1996), and our own *in vitro* studies with intact bulbs support this observation (Dieudonne *et al.*, 2000).

If the main effect of LOT stimulation was to activate GC IPSPs onto secondary dendrites, why were they effective for reducing $[\text{Ca}^{2+}]$ transients in the distal apical tuft? In mammals, at least the tuft is estimated to be of the order of one length constant or less from the soma, so significant passive invasion of the IPSP should occur.

Although the measured hyperpolarization is only 10–15 mV at the soma, the GABA_A-mediated shunting Cl⁻ current would tend to stabilize the membrane potential towards rest. This would reduce [Ca²⁺] influx by limiting voltage dependent calcium channel (VDCC) currents and may reduce conductance through NMDA-R-gated channels by maintaining voltage-dependent block. Even if the Na⁺ action potential-evoked [Ca²⁺] transient in tufts of frogs is small, IPSC suppression of Na⁺ action potential initiation could have strong effects on tuft Δ[Ca²⁺] if there is synergistic interaction between the NMDA-R component of the odour-evoked synaptic potential and back-propagating spikes (Markram *et al.*, 1995) or Ca²⁺ spike generation (Bhalla & Bower, 1993). Thus, inhibitory synaptic inputs from GCs in the external plexiform layer could potentially regulate the strength of both synaptic input and output at the distal tuft.

We saw that large, long-lasting Ca²⁺ transients were evoked in tufts in subsets of glomeruli with odour stimulation, while even strong ON shock produced more moderate transients in a large number of tufts. Convergence by sensory afferents responsive to the ligand(s) of an odour onto specific glomeruli (Ressler *et al.*, 1994) provides a mechanism for strong activation of localized sets of MCs by an odour, while ON shock provides a less selective input across many glomeruli. Selective synaptic input to a subset of glomeruli favours activation of voltage-sensitive NMDA-Rs and VDCC by concentrating excitation onto MCs in the excited glomerulus and simultaneously reducing nonspecific lateral inhibition from both the glomerular and external plexiform layers. The large Ca²⁺ transient in MC tufts in glomeruli targeted by afferents sensitive to a particular odour might implement lateral inhibition by directly releasing transmitter or by facilitating action potential-mediated release to excite PG interneurons that project to adjacent, less strongly activated glomeruli. A large odour-evoked Ca²⁺ influx may thereby contribute significantly to sharpening odour discrimination by MCs by supporting a 'winner-takes-all' strategy at the distal dendritic tufts.

Odour specificity

We did not explore the issue of odour specificity of tufts in detail in this study, but we regularly observed response specificity to different odours with respect to the amplitude and timing of onset of Ca²⁺ transients in tufts in adjacent glomeruli. While more needs to be done, particularly to examine whether all tufts within the same glomerulus show the same sensitivity to different odours or to different odour concentrations, our study indicates that experiments designed to simultaneously image tufts to look for 'spatial' patterns relating to different odours should have spatial resolution sufficient to differentiate individual glomeruli. The differences in onset of up to several hundreds of milliseconds between different tufts responding to the same odour, and for the same tuft responding to different odours, indicate that the temporal resolution of intrinsic imaging techniques (Rubin & Katz, 1999) may not be sufficient to evaluate this aspect of odour processing. The extent to which the anatomical specificity of sensory afferent inputs to a tuft interacts with the activation of bulbar circuitry to sharpen the response specificity of MCs, is unknown, but potentially can be studied using a preparation that has MC tufts and sensory afferents labelled with spectrally separable Ca²⁺ indicators.

Acknowledgements

This work was supported by the Canadian Institutes for Health Research and B.C. Health Research Foundation grants to K.D. and an NSERC Canada Postgraduate Fellowship to I.D. Ben Hall kindly provided data for Fig. 10B and C.

Abbreviations

ACSF, artificial cerebrospinal fluid; AMPA, α-amino-3-hydroxy-5-methyl-4-isoxazolepropionic acid; AP5, 2-amino-5-phosphonopentanoic acid; APV, DL-2-amino-5-phosphonoveralate; [Ca²⁺], Ca²⁺ concentration; CNQX, 6-cyano-7-nitroquinoxaline-2,3-dione; EPSP, excitatory postsynaptic potential; ΔF/F, fractional fluorescence change; GC, granule cell; IPSP, inhibitory postsynaptic potential; LFP, local field potential; LOT, lateral olfactory tract; MC, mitral cell; NMDA, N-methyl-D-aspartate; OB, olfactory bulb; ON, olfactory nerve; ORN, olfactory receptor neuron; PG, periglomerular cell; TPLSM, two-photon laser scanning microscopy.

References

- Adrian, E.D. (1942) Olfactory reactions in the brain of the hedgehog. *J. Physiol. (Lond)*, **100**, 459–473.
- Aroniadou-anderjaska, V., Ennis, M. & Shipley, M.T. (1997) Glomerular synaptic responses to olfactory nerve input in rat olfactory bulb slices. *Neuroscience*, **79**, 425–434.
- Aroniadou-anderjaska, V., Ennis, M. & Shipley, M.T. (1999) Dendrodendritic recurrent excitation in mitral cells of the rat olfactory bulb. *J. Neurophysiol.*, **82**, 489–494.
- Bardoni, R., Magherini, P.C. & Belluzzi, O. (1996) Excitatory synapses in the glomerular triad of frog olfactory bulb *in vitro*. *Neuroreport*, **7**, 1851–1855.
- Berkowicz, D.A., Trombley, P.Q. & Shepherd, G.M. (1994) Evidence for glutamate as the olfactory receptor cell neurotransmitter. *J. Neurophysiol.*, **71**, 2557–2561.
- Bhalla, U.S. & Bower, J.M. (1993) Exploring parameter space in detailed single neuron models: simulations of the mitral and granule cells of the olfactory bulb. *J. Neurophysiol.*, **69**, 1948–1965.
- Bischofberger, J. & Jonas, P. (1997) Action potential propagation into the presynaptic dendrites of rat mitral cells. *J. Physiol. (Lond)*, **504**, 359–365.
- Bozza, T.C. & Kauer, J.S. (1998) Odorant response properties of convergent olfactory receptor neurons. *J. Neurosci.*, **18**, 4560–4569.
- Buonviso, N. & Chaput, M.A. (1990) Response similarity to odors in the olfactory bulb output cells presumed to be connected to the same glomerulus: electrophysiological study using simultaneous single-unit recordings. *J. Neurophysiol.*, **63**, 447–454.
- Carlson, G.C., Shipley, M.T. & Keller, A. (2000) Long-lasting depolarizations in mitral cells of the rat olfactory bulb. *J. Neurosci.*, **20**, 2011–2021.
- Charpak, S., Mertz, J., Moreaux, L., Beaupaire, E. & Delaney, K.R. (2001) Two-photon imaging of odor-evoked Ca²⁺ dynamics in dendritic compartments of rat mitral cells. *Proc. Natl. Acad. USA*, **98**, 1230–1234.
- Chen, W.R., Midtgaard, J. & Shepherd, G. (1997) Forward and backward propagation of dendritic impulses and their synaptic control in mitral cells. *Science*, **278**, 463–467.
- Chen, W.R., Xiong, W. & Shepherd, G. (2000) Analysis of relations between NMDA receptors and GABA release at olfactory bulb reciprocal synapses. *J. Neuron*, **25**, 625–633.
- Cinelli, A.R., Hamilton & K.A.Kauer, J.S. (1995) Salamander olfactory bulb neuronal activity observed by video rate, voltage-sensitive dye imaging III. Spatial and temporal properties of responses evoked by odorant stimulation. *J. Neurophysiol.*, **73**, 2053–2071.
- Davison, I.G. & Delaney, K.R. (1997) Pharmacology of odor-evoked calcium transients in mitral cell apical dendritic tufts. *Soc. Neurosci. Abstr.*, **23**, 1271.
- Davison, I.G. & Delaney, K.R. (1998) Control of odor-induced Ca²⁺-influx in mitral cell apical dendritic tufts. *Soc. Neurosci. Abstr.*, **24**, 78.
- Davison, I.G. & Delaney, K.R. (2000) Control of odor response properties in mitral cells of the vertebrate olfactory bulb. *Soc. Neurosci. Abstr.*, **26**, 1478.
- Delaney, K.R. & Denk, W. (1996) Dynamics of odor-induced Ca²⁺ changes in mitral cell apical tufts. *Soc. Neurosci. Abstr.*, **22**, 2021.
- Delaney, K.R. & Hall, B.J. (1996) An *in vitro* preparation of frog nose and brain for the study of odour-evoked oscillations. *J. Neurosci. Meth.*, **68**, 193–202.
- Denk, W. & Svoboda, K. (1997) Photon upmanship: why multiphoton imaging is more than a gimmick. *Neuron*, **18**, 351–357.
- Denk, W., Piston, D.W. & Webb, W.W. (1995) Two-photon molecular excitation in laser scanning microscopy. In Pawley, J. (ed.), *The Handbook of Confocal Microscopy*, 2nd edn. Plenum, New York, NY, pp. 445–458.
- Denk, W., Strickler, J.H. & Webb, W.W. (1990) Two-photon laser scanning fluorescence microscopy. *Science*, **248**, 73–76.
- Denk, W. (1996) Two photon excitation in functional biological imaging. *J. Biomed Opt.*, **1**, 296–304.

- Dieudonne, S., Kehoe, J. & Delaney, K.R. (2000) Dendritic integration in periglomerular cells of the olfactory bulb. *Soc. Neurosci. Abstr.*, **26**, 1626.
- Duchamp-Viret, P., Duchamp, A. & Chaput, M.A. (2000) Peripheral odor coding in the rat and frog: Quality and intensity specification. *J. Neurosci.*, **20**, 2383–2396.
- Duchamp-Viret, P., Duchamp, A. & Vigouroux, M. (1990) Temporal aspects of information processing in the first two stages of the frog olfactory system: influence of stimulus intensity. *Chem. Senses*, **15**, 346–365.
- Emptage, N., Bliss, T.V. & Fine, A. (1999) Single synaptic events evoke NMDA receptor-mediated release of calcium from internal stores in hippocampal dendritic spines. *Neuron*, **22**, 115–124.
- Ennis, M., Zimmer, L.A. & Shipley, M.T. (1996) Olfactory nerve stimulation activates rat mitral cells via NMDA and non-NMDA receptors *in vitro*. *Neuroreport*, **7**, 989–992.
- Freeman, W.J. (1974) Attenuation of transmission through glomeruli of olfactory bulb on paired shock stimulation. *Brain Res.*, **65**, 77–90.
- Friedrich, R.W. & Korsching, S.I. (1997) Combinatorial and chemotopic odorant coding in the zebrafish olfactory bulb visualized by optical imaging. *Neuron*, **18**, 737–752.
- Gelperin, A. & Flores, J. (1997) Vital staining from dye-coated microprobes identifies new olfactory interneurons for optical & electrical recording. *J. Neurosci. Meth.*, **72**, 97–108.
- Getchell, T.V. (1986) Functional properties of vertebrate olfactory receptor neurons. *Physiol. Rev.*, **66**, 772–818.
- Getchell, T.V. & Shepherd, G.M. (1975) Short-axon cells in the olfactory bulb: dendrodendritic synaptic interactions. *J. Physiol. (Lond)*, **251**, 523–548.
- Getchell, T.V. & Shepherd, G.M. (1978) Adaptive properties of olfactory receptors analysed with odour pulses of varying durations. *J. Physiol. (Lond)*, **282**, 541–560.
- Graubard, K., Raper, J.A. & Hartline, D.K. (1980) Graded synaptic transmission between spiking neurons. *PNAS*, **77**, 3733–3735.
- Halabisky, B., Friedman, D., Radojicic, M. & Strowbridge, B.W. (2000) Calcium influx through NMDA receptors directly evokes GABA release in olfactory bulb granule cells. *J. Neurosci.*, **20**, 5124–5134.
- Hobson, J.A. (1967) Respiration and EEG synchronization in the frog. *Nature*, **11**, 988–989.
- Isaacson, J.S. (1999) Glutamate spillover mediates excitatory transmission in the rat olfactory bulb. *Neuron*, **23**, 377–384.
- Isaacson, J.S. & Strowbridge, B.W. (1998) Olfactory reciprocal synapses: dendritic signaling in the CNS. *Neuron*, **20**, 749–761.
- Jahr, C.E. & Nicoll, R.A. (1981) Primary afferent depolarization in the *in vitro* frog olfactory bulb. *J. Physiol. (Lond)*, **318**, 375–384.
- Jahr, C.E. & Nicoll, R.A. (1982) An intracellular analysis of dendrodendritic inhibition in the turtle *in vitro* olfactory bulb. *J. Physiol. (Lond)*, **326**, 213–234.
- Jiang, T. & Holley, A. (1992a) Morphological variations among output neurons of the olfactory bulb in the frog (*Rana ridibunda*). *J. Comp. Neurol.*, **320**, 86–96.
- Jiang, T. & Holley, A. (1992b) Some properties of receptive fields of olfactory mitral/tufted cells in the frog. *J. Neurophysiol.*, **68**, 726–733.
- Keller, A., Yagodin, S., Aroniadou-Anderjaska, V., Zimmer, L.A., Ennis, M., Sheppard, N.F. & Shipley, M.T. (1998) Functional organization of rat olfactory bulb glomeruli revealed by optical imaging. *J. Neurosci.*, **18**, 2602–2612.
- Kirillova, V. & Lin, J.W. (1998) A whole-cell clamp study of dendrodendritic synaptic activities in mitral cells of turtle olfactory bulb slices. *Neuroscience*, **87**, 255–264.
- Lam, Y.W., Cohen, L.B., Wachowiak, M. & Zochowski, M.R. (2000) Odors elicit three different oscillations in the turtle olfactory bulb. *J. Neurosci.*, **20**, 749–762.
- Laurent, G. (1993) A dendritic gain control mechanism in axonless neurons of the locust, *Schistocerca americana*. *J. Physiol. (Lond)*, **470**, 45–54.
- Markram, H., Helm, P.J. & Sakmann, B. (1995) Dendritic calcium transients evoked by single back-propagating action potentials in rat neocortical pyramidal neurons. *J. Physiol. (Lond)*, **485**, 1–20.
- Matsui, K., Hosoi, N. & Tachibana, M. (1999) Active role of glutamate uptake in the synaptic transmission from retinal nonspiking neurons. *J. Neurosci.*, **19**, 6755–6766.
- Mori, K., Nowycky, M. & Shepherd, G.M. (1982) Impulse activity in presynaptic dendrites: analysis of mitral cells in the isolated turtle olfactory bulb. *J. Neurosci.*, **2**, 497–502.
- Mori, K., Nowycky, M. & Shepherd, G.M. (1984) Synaptic excitatory and inhibitory interactions at distal dendritic sites on mitral cells in the isolated turtle olfactory bulb. *J. Neurosci.*, **4**, 2291–2296.
- Nickell, W.T., Shipley, M.T. & Behbehani, M.M. (1996) Orthodromic synaptic activation of rat olfactory bulb mitral cells in isolated slices. *Brain Res. Bull.*, **39**, 57–62.
- Nowycky, M., Mori, K. & Shepherd, G.M. (1981) Blockade of synaptic inhibition reveals long-lasting synaptic excitation in isolated turtle olfactory bulb. *J. Neurophysiol.*, **46**, 649–658.
- Puopolo, M. & Belluzzi, O. (1998) Inhibitory synapses among interneurons in the glomerular layer of rat and frog olfactory bulbs. *J. Neurophysiol.*, **80**, 344–349.
- Rall, W. & Shepherd, G.M. (1968) Theoretical reconstruction of field potentials and dendro-dendritic synaptic interactions in olfactory bulb. *J. Neurophysiol.*, **31**, 884–915.
- Ressler, K.J., Sullivan, S.L. & Buck, L.B. (1994) Information coding in the olfactory system: Evidence for a stereotyped and highly organized epitope map in the olfactory bulb. *Cell*, **79**, 1245–1255.
- Rospars, J.-P., Lansky, P., Vaillant, J., Duchamp-Viret, P. & Duchamp, A. (1994) Spontaneous activity of first- and second-order neurons in the frog olfactory system. *Brain Res.*, **662**, 31–44.
- Rubin, B.D. & Katz, L.C. (1999) Optical imaging of odorant representations in the mammalian olfactory bulb. *Neuron*, **23**, 499–511.
- Scalia, F., Gallousis, G. & Roac, S.A. (1991) A note on the organization of the amphibian olfactory bulb. *J. Comp. Neurol.*, **305**, 435–442.
- Schild, D. & Riedel, H. (1992) Significance of glomerular compartmentalization for olfactory coding. *Biophys. J.*, **61**, 704–715.
- Schoppa, N.E., Kinzie, J.M., Sahara, Y., Segerson, T.P. & Westbrook, G.L. (1998) Dendrodendritic inhibition in the olfactory bulb is driven by NMDA receptors. *J. Neurosci.*, **18**, 6790–6802.
- Shepherd, G.M. & Greer, C.A. (1990) The olfactory bulb. In Shepherd, G.M. (ed.), *The Synaptic Organization of the Brain*. Oxford University Press, New York, NY, pp. 133–169.
- Tank, D.W., Delaney, K.R. & Regehr, W.G. (1995) A quantitative analysis of presynaptic calcium dynamics that contribute to short-term enhancement. *J. Neurosci.*, **15**, 7940–7952.
- Tank, D.W., Kleinfeld, D. & Gelperin, A. (1994) Olfactory oscillations, does it all compute? *Science*, **265**, 1819–1820.
- Trotter, D. & Døving, K.B. (1996) Functional role of receptor neurons in encoding olfactory information. *J. Neurobiol.*, **30**, 58–66.
- Vassar, R., Chao, S.K., Sticheran, R., Nuñez, J.M., Vosshall, L.B. & Axel, R. (1994) Topographic organization of sensory projections to the olfactory bulb. *Cell*, **79**, 981–991.
- Wellis, D.P. & Scott, J.W. (1990) Intracellular responses of identified rat olfactory bulb interneurons to electrical and odor stimulation. *J. Neurophysiol.*, **64**, 932–947.